JOURNAL OF MORPHOLOGY 268:844–865 (2007)

Cranial Endocasts From a Growth Series of *Monodelphis domestica* (Didelphidae, Marsupialia): A Study of Individual and Ontogenetic Variation

Thomas E. Macrini,[1]* Timothy Rowe,[2,3] and John L. VandeBerg[4]

[1]*Department of Mammalogy, American Museum of Natural History, New York, New York 10024*
[2]*Jackson School of Geosciences, The University of Texas at Austin, Austin, Texas 78712*
[3]*University of Texas High-Resolution X-ray Computed Tomography Facility, The University of Texas at Austin, Austin, Texas 78712*
[4]*Southwest Foundation for Biomedical Research, P.O. Box 760549, San Antonio, Texas 78245*

ABSTRACT Intraspecific variation (e.g., ontogenetic, individual, sexual dimorphic) is rarely examined among cranial endocasts (infillings of the braincase cavity) because of the difficulty in obtaining multiple specimens of a species, particularly fossil taxa. We extracted digital cranial endocasts from CT scans of a growth series of skulls of *Monodelphis domestica*, the gray short-tailed opossum, as a preliminary assessment of the amount of intraspecific variation in mammalian endocranial morphology. The goals of this study were 1) to provide an anatomical description to document developmental changes in endocranial morphology of *M. domestica* and 2) to examine ontogenetic and individual variation with respect to phylogenetic characters of endocranial cavities that are known to be variable between different mammalian taxa. In this study, "ontogenetic variation" refers to variation between specimens of different ages whereas "individual variation" (i.e., polymorphism) is restricted to variation between specimens of comparable age. Aside from size, changes in shape account for the greatest amount of morphological variation between the endocasts of different ages. Endocast length, width, and volume increase with age for the growth series. Relative olfactory bulb cast size increases with age in the growth series, but the relative size of the parafloccular casts shows a slight negative allometric trend through ontogeny. More than one-third of the phylogenetic characters of the endocranial cavity we examined showed some sort of variation (ontogenetic, individual, or both). This suggests that although endocasts are potentially informative for systematics, both ontogenetic and individual variation affect how endocranial characters are scored for phylogenetic analysis. Further studies such as this are necessary to determine the taxonomic extent of significant intraspecific variation of these endocranial characters. J. Morphol. 268:844–865, 2007.

KEY WORDS: cranial endocast; opossum; polymorphism; intraspecific variation; computed tomography

Cranial endocasts (sensu Colbert et al., 2005; Macrini et al., 2006, 2007a) are three-dimensional representations of the space within the cranial cavity (i.e., endocranial space), which is filled primarily by the brain in vivo. Soft tissue structures, such as organs, only fossilize under extraordinary conditions, as was the case with frozen Pleistocene mammals from northern Russia and Alaska (Farrand, 1961; Guthrie, 1990). Because of the extreme rarity of this type of soft tissue preservation, paleontologists rely mostly on cranial endocasts to study the brain and associated sensory systems in extinct animals. This branch of paleontology dealing with the fossil record of the nervous system is known as paleoneurology (Jerison, 1973; Buchholtz and Seyfarth, 1999).

Cranial endocasts provide better approximations of the brains of some vertebrates than others based on the degree to which the brain fills the endocranial space (Jerison, 1973). The brains of mammals largely fill the endocranial space leaving impressions of gross structures on the internal surfaces of skull bones. Because of this, the importance of cranial endocasts for studying the evolution of the brain in fossil mammals has long been recognized (e.g., Marsh, 1884; Simpson, 1927, 1937; Edinger, 1942, 1948, 1949, 1955, 1964, 1975; Radinsky, 1968a,b, 1973a,b, 1976, 1977; Jerison, 1973, 1991; Kielan-Jaworowska, 1983, 1984, 1986; Rowe, 1996a,b).

Comparisons of the relative sizes of gross structures of the brains of extant animals are used to infer the degree of evolution of different sensory systems (Jerison, 1973; Butler and Hodos, 1996). This is based on the "principle of proper mass"

Contract grant sponsor: National Science Foundation; Grant numbers: IIS 0208675, DEB 0309369; Contract grant sponsors: Kalbfleisch/Lincoln Ellsworth Research Fellowship at AMNH, Robert J. Kleberg, Jr. and Helen C. Kleberg Foundation.

*Correspondence to: Thomas E. Macrini, Department of Mammalogy, American Museum of Natural History, Central Park West at 79th Street, New York, NY 10024. E-mail: tmacrini@amnh.org

Published online 11 July 2007 in
Wiley InterScience (www.interscience.wiley.com)
DOI: 10.1002/jmor.10556

which states that the mass of the neural tissue of a particular segment of the brain is correlated with the amount of information processing involved in performing that particular function (Jerison, 1973:8). A related assumption, based on observations on extant mammals, is that gross structures of cranial endocasts of mammals provide reasonable proxies for the size of the corresponding brain feature (Edinger, 1948; Jerison, 1973). Therefore, comparative studies of different portions of endocasts of extinct and extant mammals provide information about the evolution of different sensory systems (e.g., Radinsky, 1968a,b, 1973a,b, 1976, 1977). For example, an endocast with relatively large superior colliculus casts suggests that this individual and presumably its species had large superior colliculi and more acute eyesight in comparison to an endocast with smaller superior colliculus casts. Studies based on these types of comparisons between regions of the cranial cavity can be crude, but endocasts are often the best available information about the central nervous system and sensory systems of extinct taxa. Endocasts do not provide any direct information about the internal structure of the brain such as morphology of the neurons, number of neurons, neuron density, or neuron connectivity. But differences in endocast shape alone are highly informative when evaluated in the context of the comparative neuroanatomy of extant mammals (Nieuwenhuys et al., 1998).

Study of the sensory systems is important for understanding the behavior of organisms. Behavior is response to stimuli and the brain is the organ in which sensory information and motor functions are primarily coordinated. The evolution of behavior is related to the evolution of the brain, and therefore cranial endocasts are useful for studying the behavior of extinct animals and the history of modern sensory systems.

In addition, cranial endocasts represent a potentially large amount of unexplored phylogenetic data. Several previous studies utilized central nervous system characters to determine phylogenetic relationships of extant animals (e.g., Johnson et al., 1982a,b; Kirsch, 1983; Kirsch and Johnson, 1983; Kirsch et al., 1983; Northcutt, 1984, 1985; Rowe, 1988; Johnson et al., 1994; Luo et al., 2001a,b, 2002, 2003; Luo and Wible, 2005). However, relatively few studies have exclusively incorporated endocranial space characters in phylogenetic analyses of extinct and extant taxa (e.g., Northcutt, 1984, 1985; Roth and Wullimann, 2001; Lyras and van der Geer, 2003; Franzosa, 2004; Kielan-Jaworowska et al., 2004; Striedter, 2005; Macrini, 2006). Internal cranial morphology such as represented by endocasts is poorly represented in phylogenetic analyses because of the difficulty in visualizing and studying this anatomy, especially in fossil taxa.

Historically, studies of the brains of fossils were restricted to those with natural endocast material or specimens from which artificial endocasts could be easily extracted using conventional methods. However, the cranial cavities of many fossil specimens are filled with matrix and their endocranial space could only be studied through destructive serial sectioning. In recent years, high-resolution X-ray computed tomography was established as a proven technology for extracting endocasts from virtually any skull, fossil or extant, in a nondestructive manner (e.g., Rowe et al., 1995; Brochu, 2000; Larsson et al., 2000; Witmer et al., 2003; Franzosa and Rowe, 2005; Macrini et al., 2006, 2007a,b). Consequently, our knowledge of the evolution of endocranial space in mammals has expanded with the study of additional extant and extinct taxa.

Even so, some basic questions about the study of endocasts remain unanswered, such as the range of intraspecific variation for a particular species. Intraspecific variation may include but is not restricted to ontogenetic, individual, and sexually dimorphic variation. In this article, "ontogenetic variation" refers to variation between individuals of different ages whereas "individual variation" is restricted to variation between individuals of comparable age (i.e., polymorphism; Wiens, 1995, 1998, 1999, 2000; Hilton and Bemis, 1999). We do not examine sexual dimorphism in this study because we lacked the appropriate sample of males and females to evaluate this type of variation at this time.

Relatively few studies of cranial endocasts have examined multiple specimens of a particular taxon to understand individual variation (notable exceptions are Edinger, 1948; Radinsky, 1968b, 1973a; Jerison, 1979; Novacek, 1982, 1986), and virtually no studies have examined ontogenetic variation of endocasts for a particular taxon. Morphological characters that show intraspecific variation are known to contain phylogenetic signal, and different treatments of these characters can greatly affect the results of phylogenetic analyses (Wiens, 1995, 1998, 1999), as well as species-level diagnoses of taxa (Bell and Gauthier, 2002; Bever, 2005; Bever et al., 2005). Therefore, it is important to assess the degree of intraspecific variation among endocasts so that characters related to this system can be properly treated in phylogenetic analyses.

To address these and other issues, we described cranial endocasts of *Monodelphis domestica*, the gray short-tailed opossum, based on multiple individuals from different ages of postnatal ontogeny. We compared these endocasts with the gross anatomy of brains of *M. domestica* that were extracted by dissection from individuals of comparable age. We also compared the endocasts of *M. domestica* with an endocast from an adult *Didelphis virginiana*, the Virginia opossum, because the gross anatomy of the brain and associated soft tissue of *D. virginiana* is well documented (Voris, 1928; Loo, 1930; Voris and Hoerr, 1932; Larsell, 1936; Krabbe, 1942;

Dom et al., 1970; Nieuwenhuys et al., 1998). The morphology of endocasts of adult *M. domestica* was compared elsewhere with an endocast of *Pucadelphys andinus*, an extinct metatherian from Bolivia (Macrini et al., 2007a). Published descriptions of endocasts of a number of other fossil metatherians (e.g., Quiroga, 1978; Haight and Murray, 1981; Quiroga and Dozo, 1988; Dozo, 1989, 1994) and descriptions of other marsupial brains (e.g., Owen, 1837; Johnson, 1977; Haight and Nelson, 1987) provide additional comparative data.

The goals of this study are as follows: 1) to document developmental changes in the morphology of cranial endocasts of *Monodelphis domestica*, and 2) to use the growth series to document ontogenetic and individual variation of phylogenetic characters of endocranial cavities that are known to be variable between different mammalian taxa. We investigated three questions related to the second goal of this study. 1) Should ontogenetic (post-organogenesis) variation be taken into consideration when studying endocasts? That is, apart from size alone is there significant ontogenetic variation such that it would affect scoring phylogenetic characters? 2) Should individual variation be taken into consideration when studying endocasts? 3) Is the brain growth trajectory for one species of mammal (*M. domestica*) different from a brain allometry trajectory based on adults from a higher taxonomic group of mammals?

MATERIALS AND METHODS

Taxonomy

In this article, the names Mammalia, Monotremata, Theria, Metatheria, Marsupialia, Eutheria, and Placentalia refer to clades with explicit phylogenetic definitions. A crown-group definition (de Queiroz and Gauthier, 1990) is used for Mammalia, such that the clade includes the most recent common ancestor (hereafter "MRCA") of Theria and Monotremata, and all descendants of that ancestor (Rowe, 1988). Mammals are members of Mammalia; the same convention is followed for the other clades discussed here. Monotremata, Marsupialia, and Placentalia are also treated as crown groups. Theria includes the MRCA between Marsupialia and Placentalia and all descendants of that ancestor (Rowe, 1988). Metatheria is a stem clade that incorporates all therians more closely related to Marsupialia than to Placentalia, including all marsupials (Rougier et al., 1998; Flynn and Wyss, 1999). Similarly, Eutheria is the stem clade that includes all therians more closely related to Placentalia than to Marsupialia, including all placentals.

Other names are used more informally, without explicit phylogenetic definitions. The term "nonmammalian cynodonts" refers to a paraphyletic assemblage of the closest extinct relatives of crown mammals. Didelphidae is the basal-most diverging clade of extant, neotropical marsupials (Jansa and Voss, 2000; Horovitz and Sánchez-Villagra, 2003; Voss and Jansa, 2003).

Taxon Choice

Monodelphis domestica (Wagner, 1842) is an appropriate taxon for this study for a number of reasons. First, *M. domestica* is a laboratory animal and therefore a growth series of specimens of known ages is easily obtainable. Second, the skull and the biology, in general, of *M. domestica* are well studied because it is a model organism for anatomical, genetic, biomedical, developmental, and evolutionary studies (e.g., Maier, 1987a,b, 1990; VandeBerg, 1990; Filan, 1991; Clark and Smith, 1993; Robinson et al., 1994; VandeBerg et al., 1994; Rowe 1996a,b; Maunz and German, 1996, 1997; Nesterova et al., 1997; VandeBerg and Robinson, 1997; Macrini, 2000, 2002, 2004; Sánchez-Villagra, 2001, 2002; Sánchez-Villagra and Sultan, 2002; Sánchez-Villagra and Wible, 2002; Sánchez-Villagra et al., 2002; Wible, 2003; Rowe et al., 2005). Finally, *M. domestica* is a member of the basal-most marsupial clade, Didelphidae (Jansa and Voss, 2000; Horovitz and Sánchez-Villagra, 2003; Voss and Jansa, 2003), and presumably approximates the most recent common ancestor of marsupials in a number of anatomical features. Therefore, results from this study might be used as a standard for variation studies of endocasts of other marsupials or even therians in general.

Specimens Examined

Endocasts and brains were extracted from *Monodelphis domestica* specimens (Table 1) obtained from the laboratory colonies of the Southwest Foundation for Biomedical Research (SFBR) in San Antonio, TX. The animals were maintained under conditions defined by VandeBerg (1999). Because these were laboratory animals, we have precise age data on the individuals. After being killed, the *M. domestica* were accessioned into the extant mammal collections of the Vertebrate Paleontology Laboratory (VPL) of The University of Texas at Austin. The VPL is an entity of the Texas Natural History Center and the specimens of the extant collections bear the prefix "TMM M." Ages of specimens are presented in days since birth, such that a "Day 90" individual is 90-days-old.

Heads or skulls of 14 individuals were CT scanned; these specimens are listed in Table 1. The sample comprises six different age classes; these are Day 27, 48, 56–57, 75–76, 90, and adult. The Day 56 and 57 individuals are considered to belong to the same age class, and similarly the Day 75 and 76 individuals are treated as comparable in age. The "adults" in this study were all sexually mature and were evaluated as a single age class, despite that they differ in age.

The material examined includes frozen, ethanol-preserved, and skeletonized specimens. Frozen and preserved specimens were dissected to extract brains. When possible, brains were extracted from individuals that were also CT scanned. In all, 10 specimens were dissected; these include two adult females, one adult male, one day 90 male, one day 76 male, one day 56 female, one day 48 female, and three day 27. The brain masses of these individuals are presented in Table 1.

The braincase of one of the Day 27 individuals (TMM M-7595) is distorted, probably a result of desiccation during skeletal preparation. Portions of the braincase roof, lateral walls, and the basicranium are collapsed. The hypophyseal fossa is damaged on this specimen and consequently a volume cannot be accurately determined for this structure.

One skull of *Didelphis virginiana* (Kerr, 1792), the Virginia opossum, (TMM M-2517; adult male collected in Travis County, Texas) was also CT scanned and its digital cranial endocast was extracted for comparison with those of *Monodelphis domestica*. This specimen has all of its adult dentition. Linear and volumetric measurement data for this particular endocast of *D. virginiana* are published elsewhere (Macrini et al., 2007a).

About CT Scanning

We used high-resolution X-ray computed tomography (HRXCT) technology to digitize skulls to extract cranial endocasts. Detailed descriptions of HRXCT are published elsewhere (Rowe et al., 1995; Denison et al., 1997; Carlson et al., 2003; <www.ctlab.geo.utexas.edu/overview/index.html>). All CT scanning of these specimens occurred at the University of Texas High-Reso-

TABLE 1. Specimens of Monodelphis domestica examined in this study

Specimen number	Preservation	Age	Sex	BdM (g)	SL (mm)	EV (mm^3)	BrM (g)
TMM M-7595	Dry skeleton	27	?	3.53[a]	18.50	248.523	?
TMM M-8265	Frozen[b]	27	?	2.85[c]	14.09	224.899	?
TMM M-8263	Ethanol	27	?	3.15[c]	?	?	0.3847
TMM M-8261	Ethanol	27	?	3.10[c]	14.04	222.982	0.0834
TMM M-7536	Dry skeleton	48	♀	12.66[d]	23.25	437.380	?
TMM M-8269	Frozen[b]	48	♀	9.70[c]	24.09	482.658	?
TMM M-8266	Frozen[b]	56	♀	15.25[c]	25.65	560.441	0.4085
TMM M-7539	Dry skeleton	57	♀	22.34[d]	25.80	486.902	?
TMM M-7542	Dry skeleton	75	♂	47.01[e]	29.20	612.469	?
TMM M-8267	Frozen[b]	76	♂	36.5[c]	30.84	689.663	0.4677
TMM M-7545	Dry skeleton	90	♀	49.36[d]	30.65	644.829	?
TMM M-8268	Frozen[b]	90	♂	54.5[c]	35.65	804.633	0.6972
TMM M-8273	Frozen	456	♂	110.0[c]	41.60	956.059	?
TMM M-8271	Frozen[b]	837	♀	89.5[c]	39.92	987.894	0.5977[f]
TMM M-7599	Dry skeleton	adult[g]	♀	80.4[h]	40.00	954.777	?
TMM M-8272	Frozen	467	♀	78.0[c]	40.55	?	0.7094
TMM M-8270	Frozen	459	♂	149.0[c]	42.35	?	?

The endocranial volumes are recorded for all individuals that were CT scanned. BdM, body mass; BrM, brain mass; EV, endocranial volume; SL, skull length.

[a]Body mass average for Day 27 determined using data from male and female individuals of laboratory colony (Table 2).

[b]Specimens were fixed in formalin and ethanol prior to brain dissection.

[c]Body mass from measurement.

[d]Body mass average for a particular age determined using data from female individuals of laboratory colony (Table 2).

[e]Body mass average for Day 75 determined using data from male individuals of laboratory colony (Table 2).

[f]Cerebellum was damaged during dissection resulting in a lower brain mass.

[g]Relative age given based on dental maturity following van Nievelt and Smith (2005).

[h]Body mass estimated using skull length vs. body mass plot (Fig. 1, Table 3).

lution X-ray CT Facility in Austin, TX (UTCT) and individual scanning parameters are documented by Macrini (2006). All specimens were scanned in their entirety through the coronal (transverse of some authors) slice plane. Frozen specimens were thawed completely prior to scanning to reduce the possibility of image artifacts associated with slippage of a thawing specimen during scanning.

Extraction of Digital Endocasts

Digital endocasts were extracted from CT scans of skulls using the program VGStudioMax© (version 1.2; Volume Graphics GmbH, 2004) and following the procedures described elsewhere (Macrini et al., 2006, 2007a). VGStudioMax© was also used to segment portions of the endocast representing distinct structures such as the olfactory bulb casts, paraflocular casts, posterior half of the cavum epiptericum casts, and hypophyseal fossa casts. The boundaries of these structures were determined following the protocols described elsewhere (Macrini et al., 2006, 2007a).

We also used VGStudioMax© to calculate volumes and partial volumes, to take linear measurements of the extracted endocast segments, and to generate movie frames of the rotating endocasts. VGStudioMax© provides measurements in microns (i.e., 0.001 mm), and these are presented verbatim here. Endocast flexure was measured following the procedure described and illustrated by Macrini et al. (2007a). Movie frames were exported to NIH ImageJ for cropping and rotation. The frames were then exported to QuickTime™ and compiled into self-contained movies. Movies of the endocasts along with CT slices of the skulls of these specimens are available on the Digimorph website <www.digimorph.org>.

Isosurface models of the endocasts were generated using VGStudioMax© and then exported to Amira 3.1™ (Zuse Institute Berlin, 2004) where the surfaces of the endocasts were smoothed for aesthetics. However, all anatomical interpretations and volume measurements were obtained prior to smoothing the endocasts to avoid the unlikely possibility that the smoothing process would significantly affect these data.

Extraction of Brains

We removed brains of specimens of *Monodelphis domestica* (Table 1) to confirm identification of anatomical features on endocasts. We used forceps to remove soft tissue of the head and pieces of the skull roofs of frozen and ethanol-preserved specimens. The neural tissue of the two frozen individuals (TMM M-8272 and TMM M-8270) that we dissected lost rigidity as the specimens thawed, making it impossible to remove intact brains from the skulls. Brain volume was recorded from a thawed brain extracted from one of the frozen specimens (TMM M-8272). However, this volume was not included in any comparisons because of potential artifacts associated with comparing brains that were preserved using different methods (Miguel and Henneberg, 1998). The remaining six frozen specimens were fixed in formalin prior to dissection. These specimens were soaked in 10% formalin for 10–12.5 days, rinsed in 95% ethanol, and then stored in 70% ethanol (Williams et al., 1977). All comparisons between endocranial volume (EV) and brain mass were conducted using these six specimens.

Extracted brains were weighed using a Mettler AE 50 scale (accurate to the nearest 0.0001 g). Skull length was measured using calipers accurate to the nearest 0.01 mm for dry skulls or by using the "distance" tool in VGStudioMax© for skulls that could not be extracted intact.

Determination of Body Mass

Frozen and whole preserved specimens were weighed using 5, 10, 30, 100, and 1,000 g Pesola spring scales with increments of 0.05, 0.1, 0.25, 1.0, and 10.0 g, respectively. Body masses were estimated for skeletonized specimens using two different techniques.

The first technique involved taking an average mass of different individuals of the same age. These mass data were taken from the LL2 stock of the laboratory colony of the SFBR; these data are provided in Table 2. The LL2 stock was selected for the robustness of its individuals and its large litter sizes (n = 10–12). This technique was applied to the nonadult skeletonized specimens. For skeletonized individuals of known sex, only

TABLE 2. Weights (g) of Monodelphis domestica collected from individuals of the LL2 stock from the Southwest Foundation for Biomedical Research in San Antonio, TX

Parents					LL2 litter weights (g)				
DAM	SIRE	Litter size	DOB	Sex	Day 27 (04/10/05)	Day 48 (05/01/05)	Day 57 (05/10/05)	Day 75 (05/28/05)	Day 90 (06/12/05)
J2501♀	J1159♂	10	03/14/05	♀	4.5	13.9	25.1	38.4	46.3
				♀	4.4	13.7	24.2	39.9	52.8
				♂	4.6	13.2	22.2	40.1	57.6
				♂	4.5	14.0	25.7	33.8	54.2
I7247♀	J1091♂	11	03/15/05		(04/11/05)	(05/02/05)	(05/11/05)	(05/29/05)	(06/13/05)
Died				♀	3.5	Maternal			
04/30/05				♀	3.1	death			
				♂	2.9				
				♂	3.3				
J0642♀	J1346♂	11	03/16/05		(04/12/05)	(05/03/05)	(05/12/05)	(05/30/05)	(06/14/05)
				♀	3.4	13.4	21.6	39.0	53.6
				♀	3.7	11.2	22.2	39.3	48.5
				♂	3.2	13.4	23.9	53.6	57.0
				♂	4.0	13.5	24.6	53.2	69.6
J0403♀	J0405♂	11	03/16/05		(04/12/05)	(05/03/05)	(05/12/05)	(05/30/05)	(06/14/05)
				♀	3.1	10.6	Litter		
				♀	3.0	10.4	death		
				♂	3.3	10.8			
				♂	2.9	10.6			
J1345♀	J8871♂	10	03/17/05		(04/13/05)	(05/04/05)	(05/13/05)	(05/31/05)	(06/15/05)
				♀	3.7	13.0	21.5	39.9	45.2
				♀	3.5	15.1	22.6	43.9	48.6
				♂	3.8	13.3	26.1	46.2	48.8
				♂	4.3	15.9	23.3	51.8	62.7
J1200♀	J3654♂	12	03/18/05		(04/14/05)	(05/05/05)	(05/14/05)	(06/01/05)	(06/16/05)
				♀	3.8	Weights	20.2	36.2	52.0
				♀	3.1	not	21.3	40.2	47.9
				♂	2.4	recorded	24.7	50.6	61.4
				♂	2.8		23.5	46.8	56.9

DAM, ID number of mother; DOB, date of birth; SIRE, ID number of father.

masses from individuals of that sex were used to determine an average mass. In the instance when the sex was unknown for the skeletonized individual (Day 27, TMM M-7595), masses from both males and females of that age were used for determining the average mass. These *Monodelphis domestica* were weighed using a Mettler PE 2000 scale (accurate to the nearest 0.1 g) at the SFBR.

A different mass estimate technique was applied to one adult opossum skeleton (TMM M-7599) because the exact age of this individual is unknown and because *Monodelphis domestica* exhibits continual growth of the long bones and overall body mass (Cothran et al., 1985; Maunz and German, 1997). The second technique estimates body mass from total skull length measured from the anterior tip of the premaxillae to the back of the occiput. Skull length was measured from adult wild-caught and laboratory-raised specimens housed in the Department of Mammalogy at the American Museum of Natural History (AMNH) in New York, NY for which body mass is known (Table 3). Skull length was measured using calipers accurate to 0.01 mm and body mass was taken from specimen tags. The skull length and body mass data were plotted and an equation for estimation of body mass was derived (Fig. 1).

Encephalization Quotients

An encephalization quotient (EQ) is a ratio of actual to expected brain sizes for a particular taxon (Jerison, 1973). These ratios are determined using plots of $\log_{10}$ (body mass) versus $\log_{10}$ (brain mass) among a number of closely related taxa.

To determine EQs in our study, $\log_{10}$ (body mass) was plotted versus $\log_{10}$ (EV) for the growth series of *Monodelphis domestica*, hereafter "growth series data set." For comparison, data from adult didelphids taken from Eisenberg and Wilson (1981), hereafter "didelphid data set," were plotted in a similar manner on the same graph. The EV data from the *M. domestica* growth series were converted to cubic cm to facilitate comparison with the adult didelphid data.

To determine an EQ equation for each data set, three types of regression analyses were performed; these include least-squares (Model 1 regression), major-axis (Model 2 regression), and reduced-major axis. Least-squares regression assumes that the *Y* variable contains error but the *X* variable does not (Sokal and Rohlf, 1998). This is an unrealistic assumption for most allometric analyses. Major-axis regression assumes that both variables have error and the variances of the two variables are equal (Sokal and Rohlf, 1998). Reduced-major axis assumes that the ratio of the two error variances equals the ratio of the actual variances of the raw data (i.e., the ratio of variance of *Y* divided by the variance of *X*; Sokal and Rohlf, 1998).

Some have advocated use of reduced-major axis for EQ analyses (e.g., Hurlburt, 1996). However, major-axis and reduced-major axis analyses can over- or underestimate the true slope if their respective assumptions are a significant departure from reality (Pagel and Harvey, 1988; Harvey and Krebs, 1990). If there is a high correlation between the *X* and *Y* variables, then all three regression methods perform well (Pagel and Harvey, 1988; Harvey and Krebs, 1990).

Quantitative data sampled from closely related taxa are non-independent (Felsenstein, 1985); therefore, the phylogenetic relationships of the didelphid data set need to be taken into account. However, the inference of a complete phylogeny for Didelphidae is still a work in progress (but see Jansa and Voss, 2000, 2005; Voss and Jansa, 2003; Jansa et al., 2006), making it difficult to determine independent contrasts for the didelphid

TABLE 3. Mass and total skull length data from wild and laboratory specimens of Monodelphis domestica

Specimen number	Sex	Mass (g)	Skull length (mm)	Specimen origin
AMNH 248302	♀	69	39.15	Wild
AMNH 133244	♂	90	39.20	Wild
AMNH 133247	♀	60	37.15	Wild
AMNH 133245	♀	50	35.25	Wild
AMNH 260024	♂	100	42.65	Wild
AMNH 261243	♀	42	34.65	Wild
AMNH 261242	♀	34	33.65	Wild
AMNH 261241	♂	53	36.20	Wild
AMNH 261240	♀	61	37.85	Wild
AMNH 261236	♂	49	37.05	Wild
AMNH 261235	♀	43	35.30	Wild
AMNH 261234	♀	33	33.95	Wild
AMNH 261233	♂	65	38.95	Wild
AMNH 261232	♀	47	34.75	Wild
AMNH 261231	♂	71	39.25	Wild
AMNH 263547	♀	70	40.30	Wild
AMNH 264481	♂	125	45.35	Laboratory
AMNH 264482	♀	92	40.20	Laboratory

AMNH, Department of Mammalogy, American Museum of Natural History in New York, NY.

data set. For this reason, independent contrasts were not analyzed for these data.

Endocranial Characters

We examined 35 morphological characters (qualitative and quantitative characters) pertaining to endocranial anatomy on the sample of 14 individuals of *Monodelphis domestica* to evaluate variation in how these characters might be scored for this taxon. These characters are part of a more extensive taxonomic study that documented their phylogenetic variation across different mammalian taxa (Macrini, 2006; Macrini et al., 2007b).

Ratio data were converted into discrete characters (Characters 2, 5, 29, 30). The remaining quantitative data were treated as discrete characters (Characters 3, 6, 19, 31, 32) by placing the data from a comparative analysis of mammalian endocasts (Macrini, 2006; Macrini et al., 2007b) into arbitrary bins and weighing the gaps between data points (e.g., segment coding; Thiele, 1993). For example, Character 3 is the angle of cranial flexure. The discrete version of this character places the angle data in bins of 5°. Letters (e.g., A, B, C, etc.) were used to designate character states when greater than 10 states were required to describe the range of variation.

We understand that conversion of quantitative data to discrete characters may not be optimal for inferring phylogenetic relationships and instead treatment of these data as continuous characters is preferred by some (articles in MacLeod and Forey, 2002). But in this article, use of segment coding is appropriate because we are assessing variability in discrete phylogenetic characters. All quantitative data for the endocasts of *Monodelphis domestica* we examined are presented in this article (Tables 1, 4, and 5) for subsequent workers who choose to treat these data as continuous characters in phylogenetic analyses.

RESULTS

Description of Endocasts

Next to size, changes in shape account for the greatest amount of morphological variation between the endocasts of the growth series of *Monodelphis domestica* (Figs. 2–5). Endocasts of younger individuals of the growth series are subspherical in overall shape when viewed dorsally, but the endocasts of the adult *M. domestica* are wedge-shaped (Figs. 2 and 3). In lateral view, the olfactory bulb casts of all of the *M. domestica* are tear drop shaped with the wider end connected to the cast of the egg-shaped cerebral hemispheres (Figs. 2 and 4).

Anteroposterior maximum length, maximum width, maximum height, and endocast flexure measurements for all 14 endocasts of *Monodelphis domestica* are presented in Table 4. Endocast length and width both increase with age for the growth series (Fig. 6). The endocast width/length aspect ratio decreases through ontogeny from 0.68–0.80 ($n = 3$) in Day 27 individuals to 0.58–0.63 ($n = 3$) in adults. Similarly, the height/length aspect ratio decreases from 0.48–0.60 ($n = 3$) in Day 27 individuals to 0.39–0.49 ($n = 3$) in adults. The endocast height/width ratio remains fairly constant throughout ontogeny (range 0.67–0.79, mean = 0.73, $n = 14$).

Endocranial volumes and brain masses of the *Monodelphis domestica* are presented in Table 1. EV increases with age in the growth series (Fig. 7).

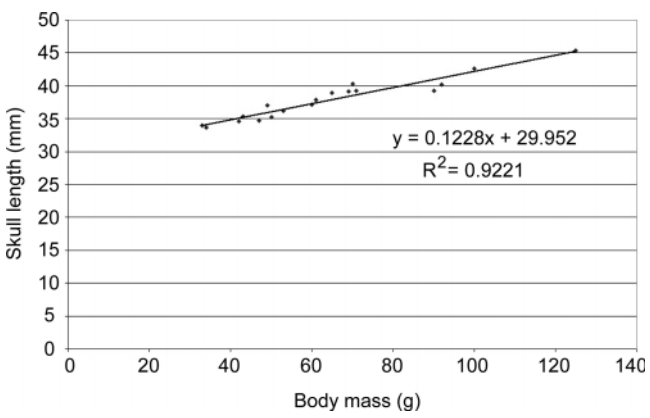

Fig. 1. Bivariate plot of total skull length (mm) vs. body mass (g) for *Monodelphis domestica*. Data for plot reported in Table 3.

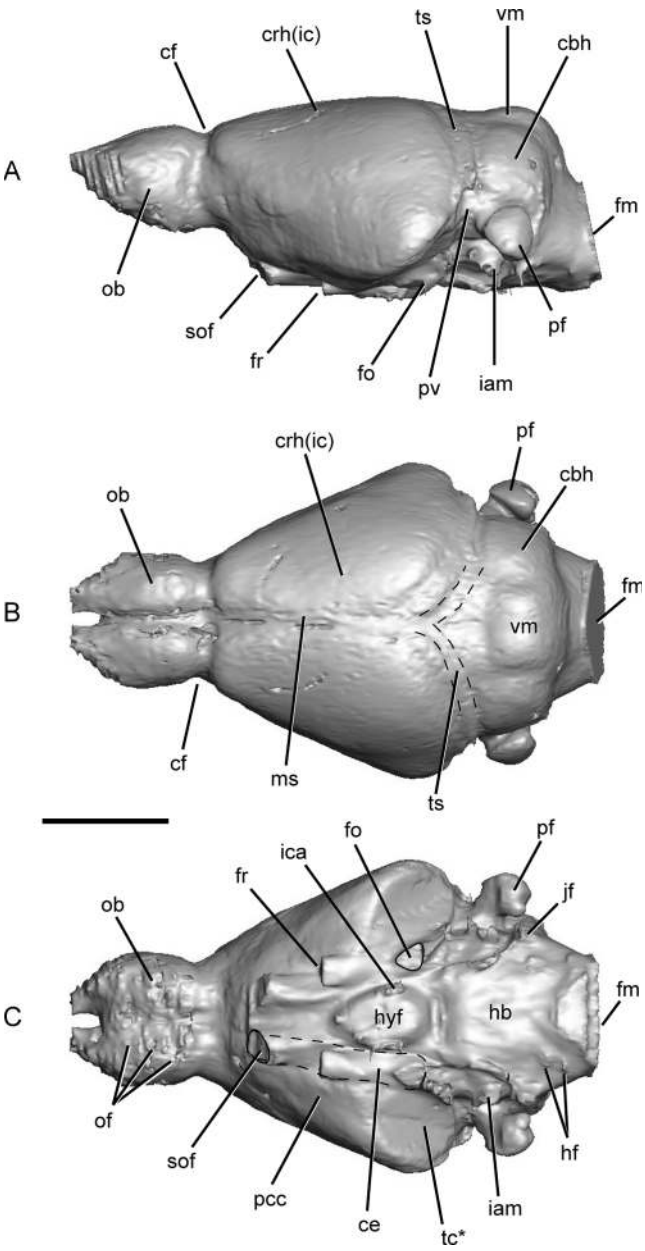

Fig. 2. Digital rendering of the cranial endocast of an adult female *Monodelphis domestica* (TMM M-7599) shown in (**A**) left lateral, (**B**) dorsal, and (**C**) ventral views. Scale bar = 5 mm. cbh, cerebellar hemisphere cast; ce, cast of cavum epiptericum (includes dashed space); cf, circular fissure; crh(ic), cast of isocortex of cerebral hemisphere; fm, foramen magnum; fo, foramen ovale (transmits cranial nerve V_3); fr, foramen rotundum (transmits cranial nerve V_2); hb, cast of hindbrain; hf, hypoglossal foramen (transmits cranial nerves XII); hyf, cast of hypophyseal fossa; iam, cast of internal acoustic meatus (transmits cranial nerves VII and VIII); ica, cast of canal that transmits the internal carotid artery; jf, jugular foramen (transmits cranial nerves IX, X, and XI); ms, median sulcus; ob, cast of olfactory bulb; of, olfactory foramen (transmits fibers of cranial nerve I); pcc, cast of piriform cortex of cerebrum; pf, paraflocular cast; pv, cast of canal that transmits prootic vein; sof, sphenorbital fissure (transmits cranial nerves II, III, IV, V_1, and VI); tc*, indentation caused by alisphenoid tympanic process; indentation marks the dorsal border of the tympanic cavity; ts, cast of transverse sinus; vm, cast of vermis.

Based on the assumption that brain tissue has a specific gravity of 1.0 g/cm^3, the brain of a Day 56 individual (TMM M-8266) of *M. domestica* fills 72.9% of the EV. The brain fills 67.8% of the EV of a Day 76 individual (TMM M-8267), and 86.6% of the EV of a Day 90 individual (TMM M-8268). Under normal physiological conditions in vivo, the cerebrospinal fluid pressure is intact and the volume of the brain is likely greater than any value obtained from a preserved specimen. Therefore the earlier values are only rough estimates of the percentage of endocranial space filled by the brain in vivo.

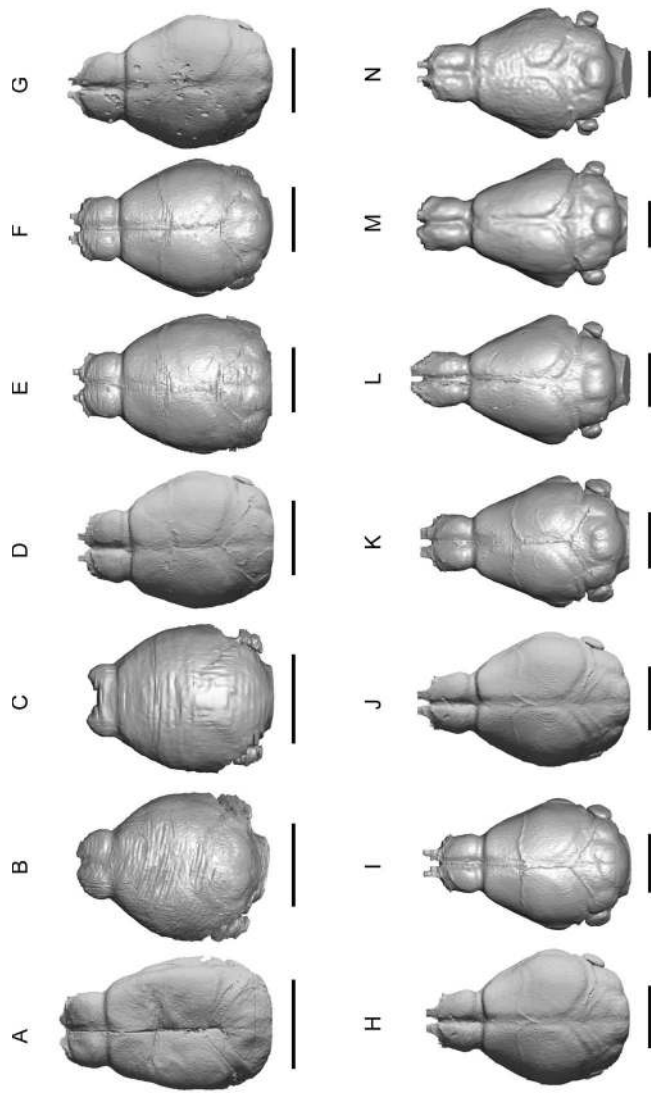

Fig. 3. Dorsal views of all endocasts of *Monodelphis domestica* used in this study. Scale bars are below each corresponding endocast image. Each scale bar = 5 mm. **A**: Day 27 (TMM M-7595). **B**: Day 27 (TMM M-8261). **C**: Day 27 (TMM M-8265). **D**: Day 48 (TMM M-7536). **E**: Day 48 (TMM M-8269). **F**: Day 56 (TMM M-8266). **G**: Day 57 (TMM M-7539). **H**: Day 75 (TMM M-7542). **I**: Day 76 (TMM M-8267). **J**: Day 90 (TMM M-7545). **K**: Day 90 (TMM M-8268). **L**: Adult female (TMM M-7599). **M**: Adult female (TMM M-8271). **N**: Adult male (TMM M-8273).

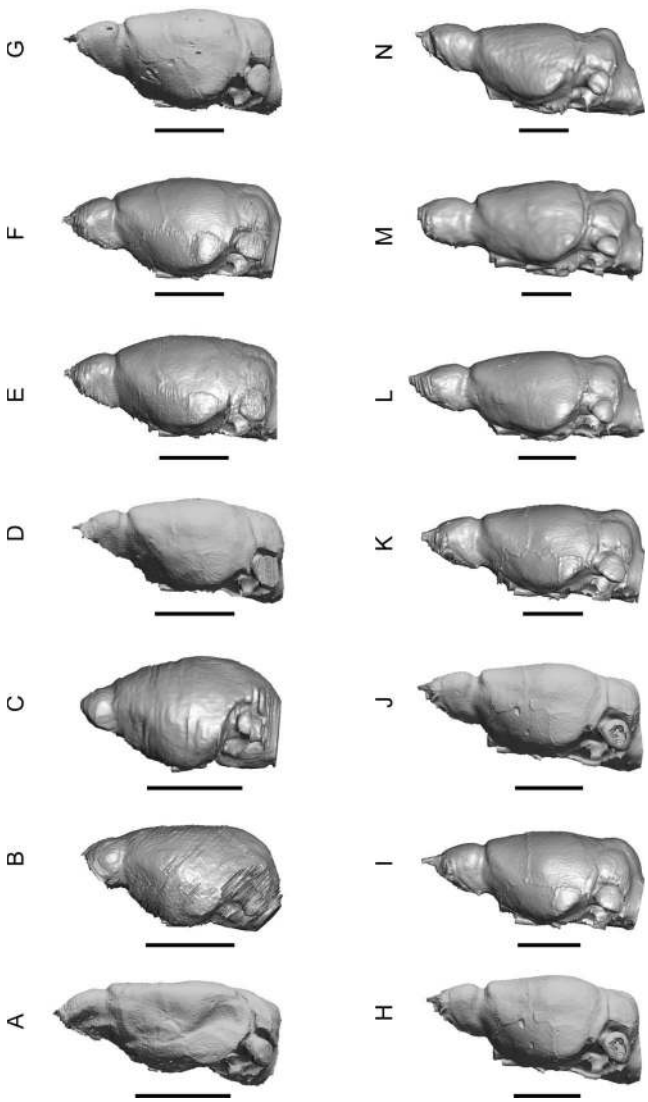

Fig. 4. Left lateral views of all endocasts of *Monodelphis domestica* used in this study. Scale bars are below each corresponding endocast image. Each scale bar = 5 mm. **A**: Day 27 (TMM M-7595). **B**: Day 27 (TMM M-8261). **C**: Day 27 (TMM M-8265). **D**: Day 48 (TMM M-7536). **E**: Day 48 (TMM M-8269). **F**: Day 56 (TMM M-8266). **G**: Day 57 (TMM M-7539). **H**: Day 75 (TMM M-7542). **I**: Day 76 (TMM M-8267). **J**: Day 90 (TMM M-7545). **K**: Day 90 (TMM M-8268). **L**: Adult female (TMM M-7599). **M**: Adult female (TMM M-8271). **N**: Adult male (TMM M-8273).

The endocast from an adult male *Didelphis virginiana* (Fig. 8) appears more laterally constricted than those of the adult *Monodelphis domestica*. The width/length aspect ratio from the endocast of *D. virginiana* is 0.57, which is near the lower range for the endocasts of the three adult *M. domestica* examined here. The tympanic cavity is relatively smaller in *D. virginiana* than in *M. domestica*, accounting for the relatively narrower endocast of *D. virginiana*. The height/length ratio of the endocast of *D. virginiana* (ratio = 0.65) is similar to those of the adult *M. domestica*, but the height/width endocast aspect ratio is considerable larger in *D. virginiana* (ratio = 1.14) than in *M. domestica*. The endocast of *D. virginiana* shows flexure of 40° around the hypophyseal cast (Macrini et al., 2007a).

Forebrain region of endocasts. The olfactory bulb casts (Fig. 2) compose 3.55–7.77% (n = 3) of endocranial space in the endocasts of the Day 27 individuals; this increases to 8.00–8.43% (n = 3) in adult *Monodelphis domestica* (Fig. 9). Younger indi-

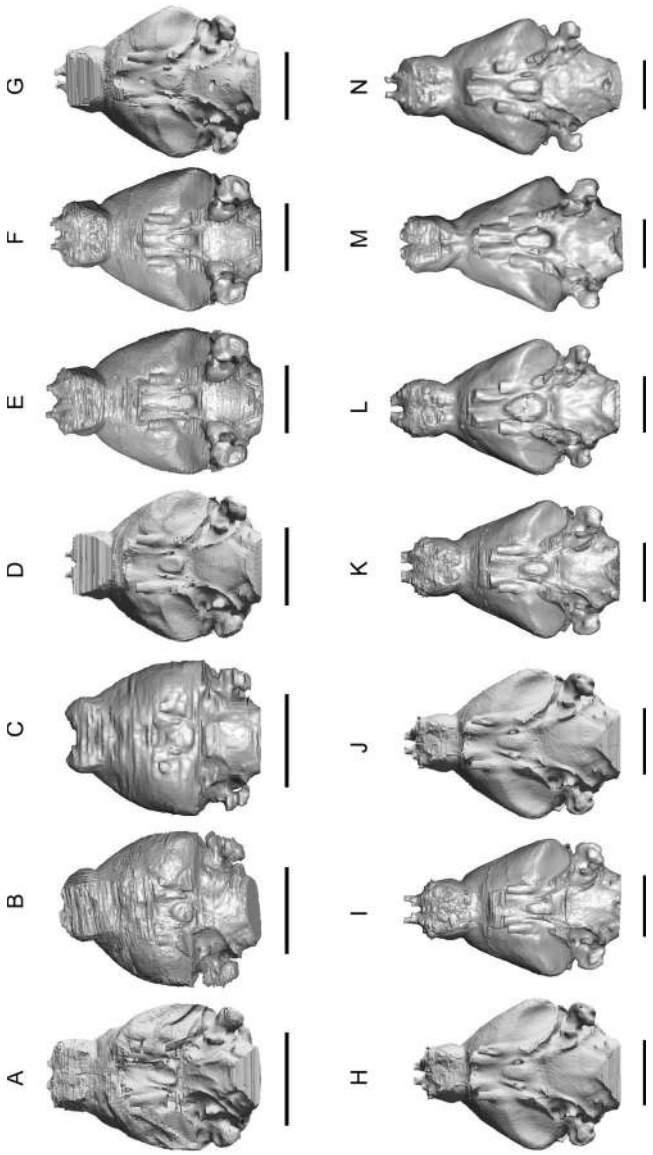

Fig. 5. Ventral views of all endocasts of *Monodelphis domestica* used in this study. Scale bars are below each corresponding endocast image. Each scale bar = 5 mm. **A**: Day 27 (TMM M-7595). **B**: Day 27 (TMM M-8261). **C**: Day 27 (TMM M-8265). **D**: Day 48 (TMM M-7536). **E**: Day 48 (TMM M-8269). **F**: Day 56 (TMM M-8266). **G**: Day 57 (TMM M-7539). **H**: Day 75 (TMM M-7542). **I**: Day 76 (TMM M-8267). **J**: Day 90 (TMM M-7545). **K**: Day 90 (TMM M-8268). **L**: Adult female (TMM M-7599). **M**: Adult female (TMM M-8271). **N**: Adult male (TMM M-8273).

TABLE 4. Linear and angle measurements taken from digital endocasts of Monodelphis domestica using VGStudioMax

Specimen number	Age	Endocast flexure	Endocast length, width, height	Olfactory bulbs length, width,[a] height	Hypophysis length, width, height
TMM M-7595	27	38°	12.020, 8.184, 5.716	2.857, 4.662, 3.101	Hypophysis damaged
TMM M-8265	27	52°	10.140, 8.125, 6.060	1.589, 4.079, 2.454	1.318, 1.456, 0.355
TMM M-8261	27	32°	10.803, 8.285, 6.520	2.097, 3.947, 2.564	1.289, 1.429, 0.415
TMM M-7536	48	42°	13.562, 10.309, 7.574	3.375, 5.195, 3.363	1.812, 1.449, 0.574
TMM M-8269	48	45°	14.515, 10.359, 7.349	3.478, 4.914, 3.852	2.058, 1.306, 0.354
TMM M-8266	56	48°	15.793, 10.868, 7.880	3.514, 5.202, 4.095	2.520, 1.306, 0.421
TMM M-7539	57	46°	14.466, 10.447, 7.916	3.853, 5.355, 4.016	1.960, 2.270, 0.582
TMM M-7542	75	37°	15.808, 11.502, 8.426	4.013, 4.999, 4.230	1.824, 2.307, 0.524
TMM M-8267	76	45°	18.200, 11.688, 8.680	5.042, 5.357, 4.641	2.737, 1.289, 0.487
TMM M-7545	90	38°	16.504, 11.986, 8.572	4.365, 5.418, 3.934	2.182, 1.855, 0.705
TMM M-8268	90	41°	19.352, 12.346, 8.680	4.850, 5.529, 4.526	3.265, 1.576, 0.430
TMM M-8273	456	38°	22.692, 13.188, 8.850	5.000, 6.014, 4.765	3.188, 2.536, 0.820
TMM M-8271	837	46°	21.105, 13.073, 9.062	5.040, 5.625, 4.792	3.780, 2.552, 0.833
TMM M-7599	Adult	46°	20.790, 13.156, 10.102	5.220, 5.747, 4.714	3.960, 3.143, 1.257

Linear measurements given in mm.
[a]Combined olfactory bulb width.

viduals of the growth series have more spherical olfactory bulb casts (Day 27 width/length aspect ratios: 0.82–1.28; $n = 3$) than those of adult specimens (width/length aspect ratios: 0.55–0.60; $n = 3$). The circular fissure (Fig. 2A) separates the olfactory bulb casts from the rest of the endocast; this fissure is well developed in all 14 endocasts of *M. domestica* and on the endocast of *Didelphis virginiana* (Fig. 8). The olfactory bulb casts constitute 11.04% of endocranial space in the specimen of *D. virginiana* examined. In *D. virginiana*, the olfactory bulb casts width/length aspect ratio (0.52) is similar to those from the adult *M. domestica*.

The anteroventral surfaces of the olfactory bulb casts of both *Monodelphis domestica* and *Didelphis virginiana* reflect the encranial surface (i.e., surface facing the endocranial cavity; Allen, 1882) of the cribriform plate of the ethmoid. The impressions of individual olfactory foramina, through which pass the fibers of cranial nerve I, are clearly visible on the endocasts (Figs. 2 and 8; Rowe et al., 2005).

Casts of olfactory tracts are not visible on any of the endocasts of *Monodelphis domestica* examined here, but they are quite conspicuous on the endocast of *Didelphis virginiana* (Fig. 8C). The olfactory tracts lead from the olfactory bulbs to the telencephalon (Butler and Hodos, 1996; Nieuwenhuys et al., 1998).

All specimens of *Monodelphis domestica* we examined have large cerebral hemisphere casts that are lissencephalic (Fig. 3). Lissencephaly is the condition of cerebral hemispheres having smooth external surfaces; that is, few gyri and sulci are visible on their exterior (Owen, 1868; Butler and Hodos, 1996; Striedter, 2005). Presumably, taxa with lissencephalic endocasts also have corresponding lissencephalic cerebral hemispheres, but this is not always the case among extant mammals (e.g.,

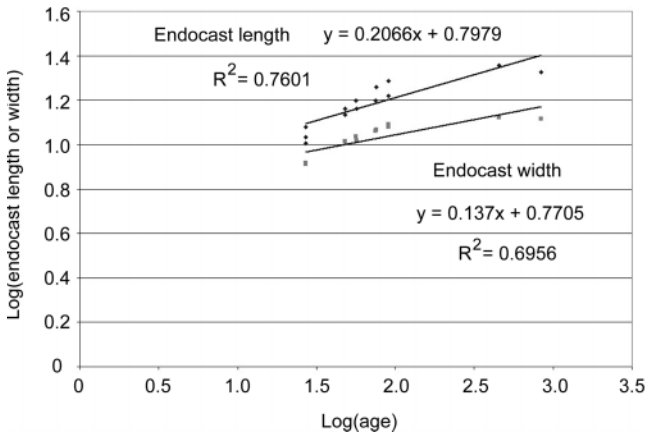

Fig. 6. Bivariate plot of $\log_{10}$(age) vs. $\log_{10}$(endocast length) and $\log_{10}$(age) vs. $\log_{10}$(endocast width) for the growth series of *Monodelphis domestica*. Note: TMM M-7599, an adult female, was not included in plot because age in days postnatal is unknown.

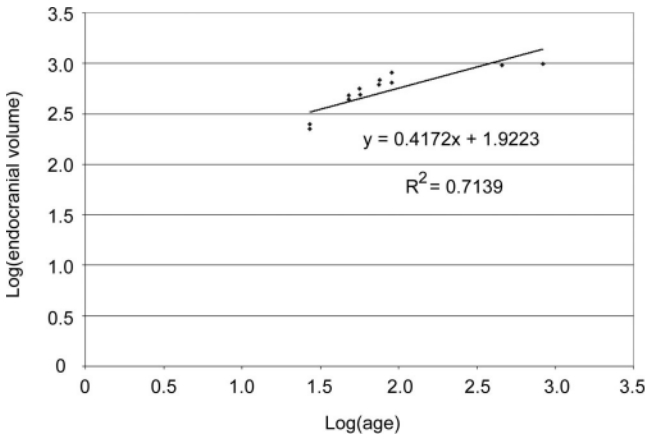

Fig. 7. Bivariate plot of $\log_{10}$(age) vs. $\log_{10}$(endocranial volume) for the growth series of *Monodelphis domestica*. Note: TMM M-7599, an adult female, was not included in plot because age in days postnatal is unknown.

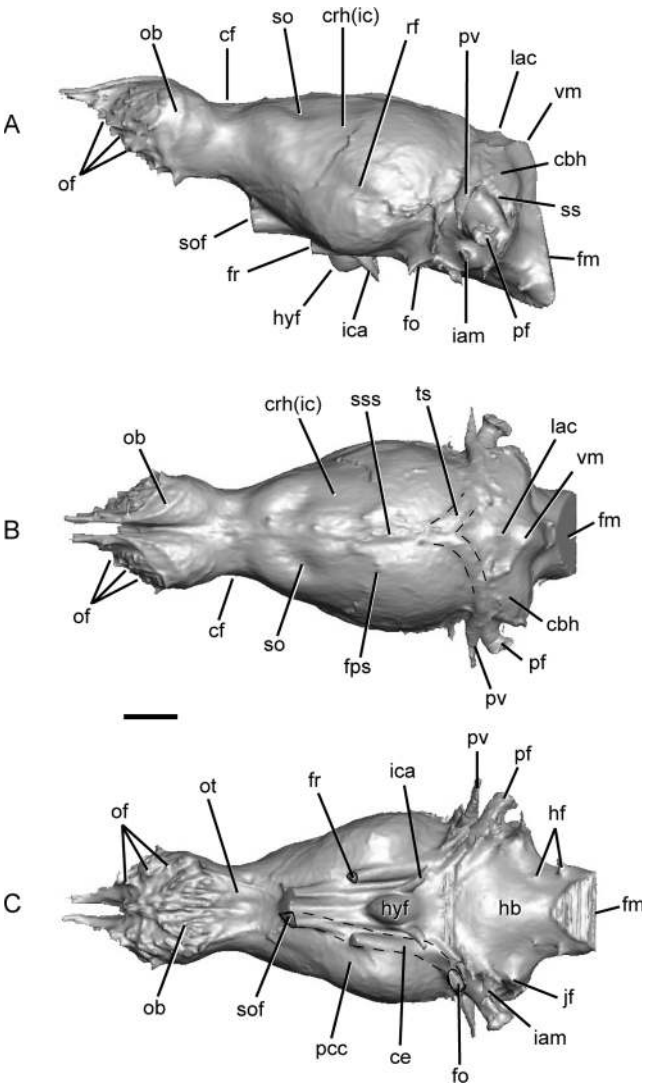

Fig. 8. Digital rendering of the cranial endocast of *Didelphis virginiana* (TMM M-2517) shown in (**A**) left lateral, (**B**) dorsal, and (**C**) ventral views. Scale bar = 5 mm. cbh, cerebellar hemisphere cast; ce, cast of cavum epiptericum (includes dashed space); cf, circular fissure; crh(ic), cast of isocortex of cerebral hemisphere; fm, foramen magnum; fo, foramen ovale (transmits cranial nerve V_3); fps, frontoparietal (coronal) suture; fr, foramen rotundum (transmits cranial nerve V_2); hb, cast of hindbrain; hf, hypoglossal foramen (transmits cranial nerves XII); hyf, cast of hypophyseal fossa; iam, cast of internal acoustic meatus (transmits cranial nerves VII and VIII); ica, cast of canal that transmits the internal carotid artery; jf, jugular foramen (transmits cranial nerves IX, X, and XI); lac, cast of lobus anterior of cerebellum; ob, cast of olfactory bulb; of, olfactory foramen (transmits fibers of cranial nerve I); ot, cast of olfactory tract; pcc, cast of piriform cortex of cerebrum; pf, parafloccular cast; pv, cast of canal that transmits prootic vein; rf, rhinal fissure; so, sulcus orbitalis; sof, sphenorbital fissure (transmits cranial nerves II, III, IV, V_1, and VI); ss, cast of canal that transmits the sigmoid sinus; sss, cast of the superior sagittal sinus; ts, cast of transverse sinus; vm, cast of vermis.

Holloway et al., 2004; Colbert et al., 2005; Shoshani et al., 2006). Dissections confirm that the cerebri of *M. domestica* are also lissencephalic (Fig. 10).

The median sulcus, which divides the cerebral hemispheres, is poorly developed on two of three endocasts of Day 27 individuals (TMM M-8261 and TMM M-8265) but is clearly visible on the remaining 12 endocasts examined in this study (Fig. 3). The rhinal fissure is not visible on any of the endocasts of *Monodelphis domestica*, but it is clearly visible on dissected brains. The rhinal fissure marks the boundary between the isocortex (or neocortex; Figs. 2 and 8; Jerison, 1991, Rowe, 1996a,b), and the piriform lobe of the cerebrum (Figs. 2 and 8). The rhinal fissure is not visible on the dissected brain of a Day 27 individual of *M. domestica* (Fig. 10) but it is visible on adult brains (fig. 1 of Brückner et al., 1998). This is consistent with the onset of isocortex development in *M. domestica* occurring during postnatal development (Saunders et al., 1989).

Several cranial sutures are visible on endocasts of the 48- to 90-day-old individuals (Figs. 3 and 4). These include the frontoparietal (coronal), alisphenoid-frontal, alisphenoid-parietal, alisphenoid-squamosal, and squamosal-parietal sutures.

The cerebrum of *Didelphis virginiana* is lissencephalic (Loo, 1930) as is the corresponding cast on the endocast (Fig. 8). The median sulcus of the endocast of *D. virginiana* is obscured by the superior sagittal sinus cast (Fig. 8B); however, the posterior portion of the rhinal fissure is visible on the lateral surface of the endocast (Fig. 8A). In addition, the sulcus orbitalis is visible on the isocortex portion of the cerebral hemisphere cast on the endocast of *D. virginiana* (Fig. 8; Nieuwenhuys et al., 1998). The frontoparietal (coronal), alisphenoid-frontal, alisphenoid-parietal, alisphenoid-squamosal, and

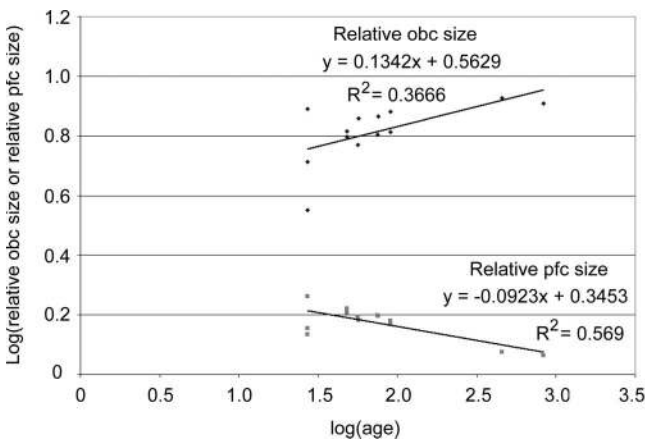

Fig. 9. Bivariate plot of $\log_{10}$(age) vs. $\log_{10}$(relative olfactory bulb cast size) and $\log_{10}$(age) vs. $\log_{10}$(relative parafloccular cast size) for the growth series of *Monodelphis domestica*. Relative size of structure refers to the percentage of the total endocranial volume composed by that particular structure. Note: TMM M-7599, an adult female, was not included in plot because age in days postnatal is unknown. obc, olfactory bulb cast; pfc, parafloccular cast.

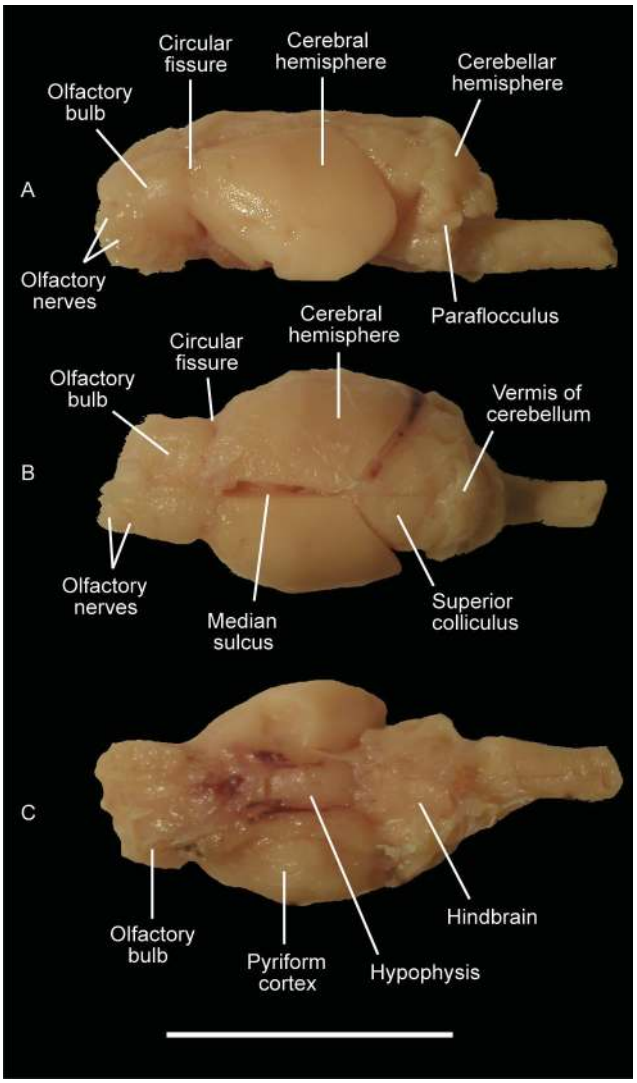

Fig. 10. Photographs of the brain of 27-day-old *Monodelphis domestica* (TMM M-8263) shown in (**A**) left lateral, (**B**) dorsal, and (**C**) ventral views. Scale bar = 1 cm.

squamosal-parietal sutures are all visible on the endocast of *D. virginiana* (Fig. 8).

Midbrain region of endocasts. The midbrain is completely obscured from the dorsal surface of the endocasts of all of the *Monodelphis domestica* examined in this study (Figs. 2 and 3). A similar condition is present in *Didelphis virginiana*, and a number of other mammals (Bauchot and Stephan, 1967; Macrini et al., 2007a). Conversely, the inferior and superior colliculi of the midbrain are visible on the dorsal surfaces of corresponding brains of *M. domestica* (Fig. 10) and *D. virginiana* (Loo, 1930; Dom et al., 1970; Nieuwenhuys et al., 1998). The large, paired transverse sinus, confluens sinuum, and associated meninges on the dorsoventral surface of the endocasts are responsible for covering the midbrain (Dom et al., 1970). The transverse sinus casts are visible on all of the endocasts of *M. domestica* examined here except for two of the Day 27 individuals (TMM M-8261 and TMM M-8265; Fig. 3). A well-developed prootic vein cast and sigmoid sinus cast are also visible anterior and dorsal (respectively) to the paraflocular casts of the Day 48–90 individuals ($n = 8$; Fig. 4). The prootic vein cast is visible on the adult endocasts but the sigmoid sinus cast is not (Figs. 2 and 4). The transverse sinus, prootic vein, and sigmoid sinus all leave impressions on the endocast of *D. virginiana* (Fig. 8).

Hindbrain region of endocasts. Casts of the vermis and cerebellar hemispheres are visible on endocasts of individuals that are at least 48-days-old ($n = 11$; Figs. 2 and 3). The cerebellum of *Monodelphis domestica* is very gyrencephalic, meaning that convolutions are visible on its exterior (Owen, 1868; Butler and Hodos, 1996; Striedter, 2005). However, the cerebellum is represented by a smooth cast on an endocast (Figs. 2–5). This indicates that the meninges and venous sinuses are covering the convolutions in a way that prevents them from embossing the overlying bones. The paraflocular casts are well developed in all individuals of this growth series (Figs. 2–5). The relative size of the paraflocular casts shows a slight negative allometric trend through ontogeny (Fig. 9), constituting 1.36–1.83% ($n = 3$) of endocranial space in Day 27 individuals and 1.10–1.19% ($n = 3$) in adults.

The casts of the vermis and cerebellar hemispheres are also visible on the endocast of *Didelphis virginiana* (Fig. 8) and, similar to *Monodelphis domestica*, meninges and cisterns (subarachnoid spaces containing cerebral spinal fluid; Butler and Hodos, 1996) cover the convolutions of the cerebellum. In addition, a cast of the lobus anterior of the cerebellum is visible anterior to the cast of the vermis on the endocast of *D. virginiana* (Fig. 8). The lobus anterior is not represented on any of the endocasts of *M. domestica*. Instead, the dorsal surfaces of the cerebellum casts of *M. domestica* (Figs. 2–4) are smooth and convex, indicating that a cistern and meninges fill the concavity between the vermis and the lobus anterior.

The paraflocular casts are small in *Didelphis virginiana* (composing 0.59% of endocranial space) relative to those of adult *Monodelphis domestica*. A cast of the internal acoustic meatus is clearly visible on the lateral surfaces of the endocasts of *M. domestica* (Figs. 2 and 5) and *D. virginiana* (Fig. 8), located just ventral and slightly anterior to the cast of the paraflocculus. The cast of the internal acoustic meatus preserves casts of the canals transmitting cranial nerves VII and VIII through the petrosal.

On the ventral surface of the endocasts of *Monodelphis domestica* (Figs. 2 and 5) and *Didelphis virginiana* (Fig. 8), the hindbrain is represented as a smooth surface because of the underlying cisterns.

The medulla oblongata and pons of the hindbrain do not leave distinctive marks on the ventral surface of any of the endocasts of *M. domestica* or *D. virginiana*. However, casts of the jugular foramen and hypoglossal foramina are visible on the ventral hindbrain casts of both of the endocasts of *M. domestica* and *D. virginiana* (Figs. 2 and 8). The jugular foramen transmits cranial nerves IX, X, and XI (Wible, 2003) and is located just posteromedial to the paraflocular cast and directly posterior to the cast of the internal acoustic meatus (Figs. 2 and 8). Two hypoglossal foramina for transmitting branches of cranial nerve XII are visible on either side of the foramen magnum in the endocasts (Figs. 2 and 8). The number of hypoglossal foramina is variable within some species of marsupials, and occasionally there is variation in number between the right and left sides of the same individual (Wible, 2003).

Midventral surface of endocasts. The cast of the hypophysis, which houses a portion of the pituitary gland, is a prominent feature in the center of the ventral surface of the endocasts of *Monodelphis domestica* (Figs. 2 and 5). The relative size of the hypophyseal fossa increases during ontogeny from composing 0.09–0.10% ($n = 2$) of endocranial space in Day 27 individuals to 0.25–0.58% ($n = 3$) of endocranial space in adults. The width/length aspect ratio of the hypophyseal fossa decreases from 1.10–1.11 ($n = 2$) in Day 27 individuals to 0.68–0.80 ($n = 3$) in adults. The depth of the hypophyseal fossa grows at a rate that is slightly slower with respect to hypophyseal length than width (height/length aspect ratio range 0.13–0.32, mean = 0.25, $n = 13$; height/width aspect ratio range 0.23–0.40, mean = 0.31, $n = 13$).

The hypophyseal cast of *Didelphis virginiana* (Fig. 8) is oval in shape (when viewed ventrally) and very deep (length = 5.544 mm; width = 4.527 mm; height = 3.336 mm), constituting 0.47% of endocranial space in *D. virginiana*. Each internal carotid artery curves anteriorly and dorsomedially to enter the posterolateral portion of the hypophyseal fossa (Fig. 8), unlike *Monodelphis domestica* in which the casts of the internal carotid arteries entering the hypophyseal fossa are straight and nearly horizontally oriented (Fig. 2).

In both *Monodelphis domestica* and *Didelphis virginiana*, the cavum epiptericum is separate from the cavum supracochleare, which sits in the petrosal and houses the geniculate ganglion of the facial nerve (Wible, 2003). The cavum epiptericum is the space between the primary and secondary walls of the braincase in mammals (Kühn and Zeller, 1987; Novacek, 1993). This space is occupied by the semilunar (Gasserian) ganglion of the trigeminal nerve (cranial nerve V), and portions of cranial nerves II–VI in *M. domestica* and *D. virginiana* (Kühn and Zeller, 1987; Maier, 1987a). The casts of the cava epipterica of *M. domestica* and *D. virginiana* are long and narrow, similar to the condition seen in the endocast of the fossil metatherian, *Pucadelphys andinus* (Figs. 2 and 8; Macrini et al., 2007a). However, the cavum epiptericum is deeper and better developed in *D. virginiana* in comparison to *M. domestica*.

A number of openings are incorporated in the cavum epiptericum space; from anterior to posterior these are the sphenorbital fissure, foramen rotundum, and the foramen ovale (Figs. 2 and 8). Several cranial nerves pass through the sphenorbital fissure of didelphids, including the optic nerve (II), the oculomotor nerve (III), the trochlear nerve (IV), a branch of the ophthalmic branch of the trigeminal nerve (V_1), and the abducent nerve (VI) (Wible, 2003). The anterior portion of the cavum epiptericum through which these nerves pass en route to the sphenorbital fissure is represented by paired canals on the endocasts (Figs. 2 and 8). The right and left casts of the cava epipterica come within close proximity to each other as they approach the fissure, but do not become completely confluent at the fissure in either *Monodelphis domestica* (Fig. 2) or *Didelphis virginiana* (Fig. 8).

The foramen rotundum (Fig. 2), for the exit of the maxillary branch of the trigeminal nerve (V_2), is located on a horizontally oriented tube that ends anterolateral to the hypophyseal cast. The foramen ovale for the exit of the mandibular branch of the trigeminal nerve (V_3) is located just posterolateral to the hypophyseal cast and sits in the posterior portion of the cavum epiptericum (Figs. 2 and 5). The foramen opens directly ventrally.

We quantified the posterior half of the cavum epiptericum, that is, the portion of the cavum that extends from the foramen rotundum posterior to the foramen ovale. This was an attempt to provide an estimate of the size of the semilunar ganglion. In *Monodelphis domestica*, the volume of both posterior halves of the cava epipterica together compose between 0.15% and 0.44% of endocranial space (mean = 0.31%, $n = 14$; Table 5). The posterior halves of the cava epipterica constitute a significantly greater percentage of the total endocranial space in older individuals (e.g., adults and Day 90) than in younger individuals (e.g., Day 27). In *Didelphis virginiana*, the posterior halves of the cava epipterica (Fig. 8) have a volume of 41.428 mm^3, which composes 0.63% of the total endocranial space.

The endocasts of *Monodelphis domestica* and *Didelphis virginiana* are nearly identical in the placement of the foramen ovale, cavum epiptericum, and orbital fissure (Figs. 2, 5, and 8). However, the distance between the orbital fissure and foramen rotundum is much greater in *D. virginiana* (Fig. 8) than in *M. domestica* (Figs. 2 and 5). The large tympanic cavity of *M. domestica* possibly accounts for the anterior displacement of the foramen rotundum (Figs. 2 and 5). The tympanic pro-

TABLE 5. Volume data taken from digital endocasts of Monodelphis domestica using VGStudioMax

Specimen number	Age	Sex	EV	OB volume[a]	PF volume[a]	HP volume	CE volume[a]
TMM M-7595	27	?	248.523	19.318	3.383	Hypophysis damaged	0.418
TMM M-8265	27	?	224.899	7.982	3.211	0.195	0.345
TMM M-8261	27	?	222.982	11.532	4.080	0.229	0.413
TMM M-7536	48	♀	437.380	27.376	7.276	0.290	1.267
TMM M-8269	48	♀	482.658	31.491	7.767	0.432	1.474
TMM M-8266	56	♀	560.441	32.928	8.752	0.407	1.440
TMM M-7539	57	♀	486.902	35.134	7.406	0.765	1.240
TMM M-7542	75	♂	612.469	38.880	9.680	0.492	2.097
TMM M-8267	76	♂	689.663	50.655	10.861	0.498	2.308
TMM M-7545	90	♀	644.829	41.925	9.549	0.541	2.724
TMM M-8268	90	♂	804.633	61.277	12.137	1.010	2.825
TMM M-8273	456	♂	956.059	80.582	11.343	2.358	4.212
TMM M-8271	837	♀	987.894	80.249	11.491	2.871	3.855
TMM M-7599	Adult[b]	♀	954.777	76.401	10.544	5.558	4.032

Absolute age given in days postnatal if known.
Volumes given in mm^3.
CE, posterior half of cavum epiptericum; EV, endocranial volume; HP, hypophyseal fossa; OB, olfactory bulb cast; PF, parafloccular cast.
[a]Volume data presented are combined for bilateral structures.
[b]Relative age given based on dental maturity following van Nievelt and Smith (2005).

cess of the alisphenoid, which forms the dorsal and anterior boundaries of the tympanic cavity, is relatively larger in *M. domestica* in comparison to *D. virginiana* resulting in a relatively larger and more anteriorly expansive tympanic cavity in *M. domestica*. The relatively large tympanic cavity accounts for a broad indentation on the posterolateral surface of the cast of the piriform lobe of the cerebrum in *M. domestica* (Fig. 2C). This indentation is absent on the endocast of *D. virginiana* (Fig. 8C).

Encephalization Quotients

The three regression methods produced similar results for the growth series of *Monodelphis domestica* (Table 6). EV is positively correlated with body mass for individuals of the growth series (Fig. 11). The three regression methods also produced similar results when the adult didelphid data of Eisenberg and Wilson (1981; hereafter referred to as the "adult didelphid data") were analyzed (Table 6). The 95% confidence intervals of the slopes of the growth series of *M. domestica* and the adult didelphid data analyses did not come close to overlapping, suggesting that the slopes of the allometry lines of the two groups are truly different (Fig. 11; Table 6). However, the datum point for the adult sample of *Monodelphis brevicaudata* from the adult didelphid data set lies on the regression line from the growth series data of *M. domestica*. The datum point for *M. brevicaudata* clusters with the data points for the adult *M. domestica*.

DISCUSSION

Endocasts and Biology of *Monodelphis domestica* During Postnatal Growth

The overall morphology of the 14 endocasts of *Monodelphis domestica* is divisible into four distinct groups. The first group consists of two of the Day 27 individuals (TMM M-8261 and TMM M-8265); the third Day 27 individual is excluded from all of the groups because desiccation of the skull resulted in a misshapen endocast. The Day 27 endocasts are characterized by relatively small, spherical olfactory bulb casts, and a large spherical "main body" of the endocast (Fig. 3).

The Day 27 individuals correspond to dental age Class 0 for which none of the upper molars are fully erupted, as assessed on cleaned skulls (van Nievelt and Smith, 2005). The onset of hearing in *Monodelphis domestica* coincides with this age. The external

TABLE 6. Results from regression analyses of the EQ plot for adult didelphid and the EQ plot for the growth series of Monodelphis domestica

Analysis	*y*-intercept	Slope	Lower CL	Upper CL
Adult didelphids				
Least-squares	−1.0488	0.6099	0.5330	0.6870
Major-axis	−1.0689	0.6187	0.5430	0.7000
Reduced-major axis	−1.0763	0.6220	0.5467	0.7048
Monodelphis domestica growth series				
Least-squares	−0.8057	0.3979	0.3410	0.4550
Major-axis	−0.8095	0.4007	0.3443	0.4593
Reduced-major axis	−0.8134	0.4037	0.3479	0.4641

Lower CL, lower bound of 95% confidence interval for the slope; upper CL, upper bound of 95% confidence interval for the slope.

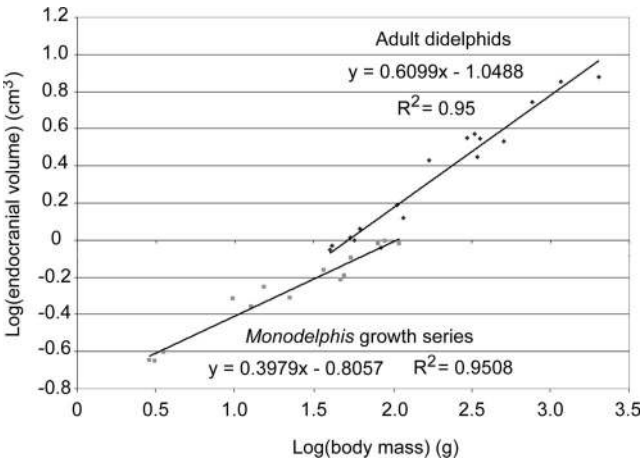

Fig. 11. Bivariate plot of the $\log_{10}$(endocranial volume) vs. $\log_{10}$(body mass) for different didelphid species (data from Eisenberg and Wilson, 1981) with data from the growth series of *Monodelphis domestica* superimposed. Endocranial volume data from the growth series were converted to cm^3.

acoustic meatus is partially open around days 28–30 postnatal (Reimer, 1996; Aitkin et al., 1997), and the middle ear ossicles are immature but are beginning to separate from the mandible (Sánchez-Villagra et al., 2002). The onset of sight also occurs around days 28–35 postnatal (Kraus and Fadem, 1987).

A number of other neurological changes associated with sensory adaptations occur shortly after Day 27. The olfactory bulbs assume an adult-like organization at the cellular level by Day 30 (Brunjes et al., 1992). The adult condition of the paraflocular lobe of the cerebellum only filling half of the subarcuate fossa is assumed by Day 35 (Sánchez-Villagra, 2002). The vomeronasal organ first opens into the nasopalatine duct by Day 40 and thus becomes functional for pheromone detection (Sánchez-Villagra, 2001).

The second morphological group of endocasts consists of Day 48 individuals. The olfactory bulb casts are relatively larger and less spherical in overall shape relative to the endocasts of Day 27 individuals (Fig. 3). By Day 48, M1 is fully erupted, corresponding to dental age Class 1 for *Monodelphis domestica* (van Nievelt and Smith, 2005).

The third morphological group is the largest and includes five individuals from Day 56 to 90. The cerebral hemisphere casts extend laterally beyond the maximum transverse extent of the cerebellar cast (Fig. 3). In this age class, the differentiation of the cerebellar cortical layers is complete by Day 75 (Sánchez-Villagra and Sultan, 2002). In addition, weaning in *Monodelphis domestica* occurs around Day 56 (Kraus and Fadem, 1987; VandeBerg, 1990). By Day 56, M2 is fully erupted, corresponding to dental age Class 2 for *M. domestica* (van Nievelt and Smith, 2005). The Day 75, 76, and 90 individuals also belong to this dental age class.

The fourth morphological group of endocasts includes one Day 90 individual (TMM M-8268) and the three adult individuals. The "main body" of the endocast, the portion posterior to the olfactory bulbs, is hexagonal in shape when viewed dorsally (Fig. 3). The flexure points between sides of the hexagon are more angular than those in endocasts of the other morphological groups.

Sexual maturity in laboratory *Monodelphis domestica* occurs at 5–6 months, and onset of reproductive decline occurs at 18–24 months in females and 24–30 months in males (VandeBerg, 1990). Individuals that die of natural causes have a lifespan of 36–42 months in captivity (VandeBerg, 1990), with a maximum documented lifespan of 49 months (Nowak, 1999). The three adult *M. domestica* used in this study correspond to the dental Class 4 because all of the adult dentition is fully erupted (van Nievelt and Smith, 2005).

Percent of Endocranial Volume Filled by the Brain in Marsupials

The brain fills 67.8–86.6% of the EV in three specimens of *Monodelphis domestica*, all from different age classes. These values fall within the range of interspecific variation for a number of Australasian marsupials including species from Dasyuridae, Peramelidae, Burramyidae, Petauridae, Pseudocheirdae, Phalangeridae, Phascolarctidae, Vombatidae, Potoroidae, and Macropodidae (Haight and Nelson, 1987).

One noteworthy taxon is the koala, *Phascolarctos cinereus*, which according to Haight and Nelson (1987), has a brain that on average only fills 61% of the EV, the lowest reported value for a mammal. A subsequent study pointed out the perils of measuring brain mass from preserved material and found that based on fresh specimens, the brain fills on average 75.8% ($n = 25$) of the EV of the koala (Miguel and Henneberg, 1998). A more recent study reported that the brain of the koala fills around 83% of the EV based on magnetic resonance imagery (MRI) of a live koala (Taylor et al., 2006). The values for the koala from the latter two studies are more in line with results from other marsupials (Haight and Nelson, 1987).

With the koala in mind, it is apparent that brain mass measurements from preserved specimens of mammals may not provide an accurate estimate for the brain mass in vivo. A difference between live and preserved brain measurements of greater than 20%, as in the koala, is an extreme case, probably because of the large size of the ventricles in this taxon (Haight and Nelson, 1987; Miguel and Henneberg, 1998; Taylor et al., 2006). Nonetheless, MRI data would provide a more accurate estimate of the percentage of EV filled by the brain in *Monodelphis domestica* and other marsupials. Such an analysis is underway for *M. domestica*.

Variation in Scoring Endocranial Phylogenetic Characters

Most of the variation observed between the endocasts of *Monodelphis domestica* is characterized as ontogenetic, although individual variation is also present in this sample. A large amount of the variation we observed is quantitative; this includes shape change as indicated by differences in aspect ratios, volume changes, and the changes in the volumes of specific structures relative to the entire EV. However, some of the variation observed here can also be characterized as qualitative.

A discussion is presented below of types or lack of variation observed in this sample of 14 endocasts of *Monodelphis domestica* for 35 endocranial characters. Reference is also made to the one endocast of *Didelphis virginiana* incorporated in this study, but obviously variation was not addressed for this taxon.

Character 1. Relative expansion of the braincase: braincase is narrow in the parietal region (0); cerebral cast expanded (the parietal part of the cranial vault is wider than the frontal part, but does not extend to lambdoidal region) (1); or greatly expanded (cerebellar cast is transversely expanded as much as cerebral cast) (2). This character was modified from Luo and Wible (2005, Character 414). Endocasts of all ages of *Monodelphis domestica* and *Didelphis virginiana* we examined have braincases that show lateral expansion but only anterior to the lambdoidal region of the endocranial cavity.

Character 2. Maximum width of entire endocast relative to its anteroposterior length: endocast longer than wide (aspect ratio < 0.9) (0); endocast length and width about equal (aspect ratio = 0.9–1.1) (1); or endocast wider than long (aspect ratio $>$ 1.1) (2). This character is from Macrini (2006; Character 2). The endocast width/length aspect ratio decreases through ontogeny, suggesting that the length of the endocranial cavity is growing at an overall faster rate than endocast width from Day 27 to adult (Rowe, 1996a). Individual variation is also noticeable between Day 27 opossums ($n = 3$) for which the endocast width/length aspect ratio has a range of 0.68–0.80. However, there is no variation in how this character is scored for *Monodelphis domestica*, based on the discrete nature of this character. All of the specimens we examined have aspect ratios less than 0.9; that is, their endocasts are longer than wide.

Character 3. Endocast flexure: 1–5° (0); 6–10° (1); 11–15° (2); 16–20° (3); 21–25° (4); 26–30° (5); 31–35° (6); 36–40° (7); 41–45° (8); 46–50° (9); 51–55° (A); or 56–60° (B). This character is from Macrini (2006; Character 6). Endocast flexure measures were rounded to the closest integer. This character shows both individual and ontogenetic variation for this sample of endocasts of *Monodelphis domestica*.

Character 4. Olfactory bulb casts: present on endocast (0); or absent from endocast (1). This character is from Macrini (2006; Character 7). All the endocasts of *Monodelphis domestica* and *Didelphis virginiana* have well-developed olfactory bulb casts.

Character 5. Width of olfactory bulb cast relative to its length: longer than wide (aspect ratio $<$ 0.9) (0); wider than long (aspect ratio $>$ 1.1) (1); or length and width are about equivalent (aspect ratio = 0.9–1.1) (2). This character is from Macrini (2006; Character 9). This character shows ontogenetic variation; younger individuals of the growth series have more spherical olfactory bulb casts than those of adult specimens. The width/length aspect ratio also varies between individuals of comparable age affecting how this character is scored for nonadult *Monodelphis domestica* (e.g., Day 27 individuals). There is no variation in how this character is scored for *M. domestica* when considering adults only.

Character 6. Percent of endocast composed by olfactory bulb casts: 0.0–0.9% (0); 1.0–1.9% (1); 2.0–2.9% (2); 3.0–3.9% (3); 4.0–4.9% (4); 5.0–5.9% (5); 6.0–6.9% (6); 7.0–7.9% (7); 8.0–8.9% (8); 9.0–9.9% (9); 10.0–10.9% (A); 11.0–11.9% (B); 12.0–12.9% (C); 13.0–13.9% (D); 14.0–14.9% (E); 15.0–15.9% (F); or 16.0–16.9% (G). This character is from Macrini (2006; Character 10). Percent data were rounded to the nearest 0.1%. This character exhibits both ontogenetic and individual variation. Relative olfactory bulb cast size increases with age in *Monodelphis domestica* as illustrated by Figure 9. Considerable variation is also noticeable between individuals of comparable age for nonadult individuals. For example, in Day 27 individuals ($n = 3$), the olfactory bulb casts constitute a range of 3.55–7.77% of endocranial space. However, there is no variation in how this character is scored for *M. domestica* when considering adults only.

Character 7. Accessory olfactory bulb casts: absent (0), or visible on endocast (1). This character is from Macrini et al. (2007b; Character 2). Accessory olfactory bulbs of extant mammals receive projections from the vomeronasal organ, which functions in the detection of pheromones (Nieuwenhuys et al., 1998). None of the endocasts of *Monodelphis domestica* or *Didelphis virginiana* that we examined had visible accessory olfactory bulb casts.

Character 8. Circular fissure (separating olfactory bulbs from cerebral hemisphere): shallow or absent (0), or deep (1) on endocast. This character is modified from Luo and Wible (2005, Character 418). A deep circular fissure is present on all endocasts of *Monodelphis domestica* and *Didelphis virginiana*. On endocasts, this fissure is a reflection of a bony annular ridge that protrudes from the internal surface of the frontal bone.

Character 9. Casts of olfactory tracts: not visible on endocast (0); or visible on endocast (1). This character is from Macrini et al. (2007b; Character 3). The casts of the olfactory tracts are not distinguishable on any of the endocasts of *Monodelphis*

domestica we examined; however, the tracts are clearly visible on the endocast of *Didelphis virginiana*.

Character 10. Lateral extent of cerebral hemisphere cast: most lateral point of cerebral cast is medial to or even with the paraflocular cast (0), or cerebral cast clearly extends laterally beyond paraflocular cast (1). This character is from Macrini et al. (2007b; Character 7). All of the endocasts of *Monodelphis domestica* exhibit state (0) for this character, but the endocast of *Didelphis virginiana* shows state (1).

Character 11. Surface of cerebral hemisphere casts: lissencephalic (i.e., smooth) (0); or gyrencephalic (i.e., convoluted) (1). This character is from Macrini et al. (2007b; Character 5). The cerebral hemisphere casts of all of the endocasts of *Monodelphis domestica* and *Didelphis virginiana* are without distinctive convolutions and are therefore considered lissencephalic. Dissections confirm that the surfaces of the cerebral hemispheres are actually lissencephalic (Fig. 10; Loo, 1930).

Character 12. Rhinal fissure on endocast: absent (0); or present (1). This character is from Macrini et al. (2007b; Character 6). None of the endocasts of *Monodelphis domestica* displays any trace of the rhinal fissure; however, the posterior portion of the fissure is visible on the endocast of *Didelphis virginiana*. The rhinal fissure marks the ventral edge of the isocortex (i.e., neocortex). Absence of this structure on an endocast does not necessarily indicate that the brain of that animal lacked an isocortex (Jerison, 1991). Dissections confirm that brains of adult *M. domestica* have a fully formed rhinal fissure (fig. 1 of Brückner et al., 1998).

Character 13. Position of rhinal fissure on endocast: on lateral surface (0); or on ventral surface (1). This character is from Macrini (2006; Character 15). This character is nonapplicable for the endocasts of *Monodelphis domestica* because they do not show the rhinal fissure. In *Didelphis virginiana*, the rhinal fissure appears on the lateral surface of the endocast.

Character 14. Exposure of midbrain (superior and inferior colliculi) on dorsal surface of endocast: absent (0); or present (1). This character is from Macrini et al. (2007b; Character 11). The midbrain is not exposed on the dorsal surface of any of the endocasts of *Monodelphis domestica* or *Didelphis virginiana*. Dissections indicate that large blood sinuses, particularly the paired transverse sinus and confluens sinuum, are responsible for obscuring the midbrain from dorsal view on endocasts (Dom et al., 1970).

Character 15. Cast of vermis of cerebellum: not visible on endocast (0); or clearly visible on endocast (1). This character is from Macrini (2006; Character 20). The vermis of the cerebellum leaves an impression on the dorsal surface of most of the endocasts of *Monodelphis domestica* and *Didelphis virginiana*. However, the vermis cast is not discernable on any of the endocasts of Day 27 individuals, probably because the cerebellum is not fully developed at this age (Sánchez-Villagra and Sultan, 2002). Studies of endocasts of the extinct multituberculate mammal *Kryptobaatar dashzevegi* suggest that the vermis is obscured by a large cistern of the subarachnoid space (Kielan-Jaworowska and Lancaster, 2004). Dissections confirm that this is certainly not the case in *Monodelphis domestica*.

Character 16. Cast of vermis of cerebellum: extends anterior to or even with the paraflocular casts (0); or vermis remains behind paraflocular casts (1). This character is modified from Luo and Wible (2005, Character 415). The vermis is located behind the paraflocular casts on all of the specimens in which the vermis is discernable on their endocast.

Character 17. Cerebellar hemisphere casts on endocast: not visible on endocast (0); or well-developed on endocast (1). This character is modified from Luo and Wible (2005, Character 417). Cerebellar hemisphere casts are visible on most endocasts of *Monodelphis domestica* and the *Didelphis virginiana*. The cerebellar hemisphere casts are not discernable on any of the endocasts of Day 27 individuals, probably because the cerebellum is not fully developed at this age (Sánchez-Villagra and Sultan, 2002).

Character 18. Cast of the paraflocculus of the cerebellum: present (0); or absent (1) on endocast. This character is from Macrini et al. (2007b; Character 14). All of the endocasts of *Monodelphis domestica* and the *Didelphis virginiana* have well-developed paraflocular casts which are representations of the space within the subarcuate fossa of the petrosal bone. It is unclear how much of this space is actually filled with the paraflocular lobe of the cerebellum. Previous studies of *M. domestica* suggest that the paraflocular lobes completely fill the subarcuate fossa early in postnatal ontogeny but only fill about half the space in adults (Sánchez-Villagra, 2002). However, the effects of desiccation of dead specimens on brain shape remain unexplored for opossums.

Character 19. Percent of endocast composed by paraflocular casts: 0.0–0.5% (0); 0.6–1.0% (1); 1.1–1.5% (2); 1.6–2.0% (3); 2.1–2.5% (4); 2.6–3.0% (5); 3.1–3.5% (6); 3.6–4.0% (7); or 4.1–4.5% (8). This character is from Macrini (2006; Character 19). Percent data were rounded to the nearest 0.1%. As mentioned earlier, the paraflocular casts are relatively larger early in the ontogeny of *Monodelphis domestica* (e.g., Day 27) than in adults (Fig. 9). This would suggest that balance and spatial orientation develop early in postnatal ontogeny because the paraflocculus is associated with these functions (Butler and Hodos, 1996). There is also some individual variation for this character; the percent of

endocranial space composed by the paraflocular casts ranges from 1.36% to 1.83% in Day 27 individuals. However, there is no variation in how this character is scored when only considering adult specimens of *M. domestica*.

Character 20. Paraflocular cast shape: cone-shaped (0), broad and rounded (1), large, posterolaterally oriented ovoids (2), or long and cylindrical without expansion on the distal end (3). This character is from Macrini et al. (2007b; Character 16). Although there is variation in the shape of the paraflocular cast in this sample of *Monodelphis domestica*, for this character all of the specimens are scored as having state (1). The specimen of *Didelphis virginiana* exhibits state (3).

Character 21. Transverse sinus cast: absent (0); or visible on endocast (1). This character is from Macrini (2006; Character 25). Transverse sinus casts are visible on all endocasts of *Monodelphis domestica* and *Didelphis virginiana* except for two of the Day 27 individuals.

Character 22. Sigmoid sinus cast: absent (0); or visible on endocast (1). This character is from Macrini (2006; Character 26). The sigmoid sinus cast is only visible on the Day 48–90 individuals of *Monodelphis domestica* and the adult *Didelphis virginiana*.

Character 23. Prootic vein cast: absent (0); or visible on endocast (1). This character is from Macrini (2006; Character 27). The prootic vein casts are visible on all of the endocasts of *Monodelphis domestica* except for the Day 27 individuals. The endocast of *Didelphis virginiana* also has a prootic vein cast.

Character 24. Superior sagittal sinus cast: visible on dorsal surface of endocast (0), or not visible (1). This character is from Macrini et al. (2007b; Character 8). The superior sagittal sinus does not leave an impression on an endocast if it is located deep within the meninges or if the walls of the sinus are completely surrounded by bone such as occurs with taxa possessing an ossified falx cerebri. The superior sagittal sinus is located within the meninges of the brain in *Monodelphis domestica* and therefore does not appear on any of the endocasts. However, this sinus leaves an impression on the dorsal surface of the endocast of *Didelphis virginiana*, effectively filling in the median sulcus so that it is not represented on the endocast (Fig. 8).

Character 25. Ossified falx cerebri: absent (0), or present (1). This character is from Macrini et al. (2007b; Character 9). The falx cerebri is a portion of the dura mater that occupies the median sulcus between the cerebral hemispheres. This osteological character is examined in this article because of the potential that it is correlated with the depth of the median sulcus on an endocast. None of the specimens of opossums we examined in this article have an ossified falx cerebri.

Character 26. Osseous tentorium: absent (0), posteromedial ossification of tentorium cerebelli (1), lateral ossification of tentorium cerebelli (2), or complete ossification of tentorium cerebelli (3). This character is from Macrini et al. (2007b; Character 10). All of the specimens of opossums we examined for this article lack any significant ossification of the tentorium cerebelli and are therefore all scored as having state (0).

Character 27. Anterior portion of cavum epiptericum leading to the sphenorbital fissure: anterior portions of right and left cava are at least partially separated at sphenorbital fissure (0), or cava are completely confluent at sphenorbital fissure (1). This character is from Macrini et al. (2007b; Character 21). The anterior portions of the right and left cava epipterica at the level of the sphenorbital fissure are in close proximity to each other but are never completely confluent in the endocasts of *Monodelphis domestica* and *Didelphis virginiana*.

Character 28. Optic chiasm: absent from endocast (0); or visible on endocast (1). This character is from Macrini (2006; Character 39). The optic chiasm is not visible on any of the endocasts of *Monodelphis domestica* or the *Didelphis virginiana*. This optic chiasm is surrounded by meninges that obscure it in the ventral view of endocasts.

Character 29. Depth of hypophyseal fossa with respect to its length: fossa deeper than long (aspect ratio > 1.1) (0); fossa longer than deep (aspect ratio < 0.9) (1); or hypophyseal fossa depth and length about equal (aspect ratio = 0.9–1.1) (2). This character is from Macrini et al. (2007b; Character 17). One of the Day 27 (TMM M-7595) exhibits state (0), but all of the other *Monodelphis domestica* show state (1).

Character 30. Width of hypophyseal fossa relative to its length: wider than long (aspect ratio $>$ 1.1) (0); longer than wide (aspect ratio < 0.9) (1); or hypophyseal length and width are about equal (aspect ratio = 0.9–1.1) (2). This character is from Macrini et al. (2007b; Character 18). The hypophyseal fossa width/length aspect ratio in *Monodelphis domestica* decreases with age indicating that as ontogeny progresses, hypophyseal length increases at a faster rate than hypophyseal width. This character also shows some individual variation for the Day 57 and Day 75 age groups.

Character 31. Percent endocast composed by hypophyseal fossa: 0.00–0.09% (0); 0.10–0.19% (1); 0.20–0.29% (2); 0.30–0.39% (3); 0.40–0.49% (4); 0.50–0.59% (5); 0.60–0.69% (6); 0.70–0.79% (7); 0.80–0.89% (8); 0.90–0.99% (9); 1.00–1.09% (A); 1.10–1.19% (B); 1.20–1.29% (C); or 1.30–1.39% (D). This character is from Macrini (2006; Character 31). Percent data were rounded to the nearest 0.01%. The relative size of the hypophyseal fossa shows ontogenetic variation in *Monodelphis domestica*; the relative size of the fossa increases with age. This agrees with the observation that the pituitary gland shows positive allometry with increasing body size across vertebrates (Edinger, 1942). This

character also shows some individual variation, especially in adults.

Character 32. Percent of endocast composed by the posterior half of the cava epipterica: 0.10–0.19% (0), 0.20–0.29% (1), 0.30–0.39% (2), 0.40–0.49% (3), 0.50–0.59% (4), 0.60–0.69% (5), 0.70–0.79% (6), 0.80–0.89% (7), 0.90–0.99% (8), 1.00–1.09% (9), 1.10–1.19% (A), 1.20–1.29% (B), or 1.30–1.39% (C). This character is modified from Macrini (2006; Character 36). Percent data were rounded to the nearest 0.01%. The relative size of the posterior half of the cavum epiptericum increases with ontogeny. The posterior portion of the cavum epiptericum is intended to be a proxy for the size of the semilunar ganglion during postnatal development. At birth, the semilunar ganglion nearly fills the cavum epiptericum of *Monodelphis domestica* and is relatively large compared with the size of the underdeveloped brain (Maier, 1987a). However, it is unclear how much of the posterior half of the cavum epiptericum is filled by the semilunar ganglion in later stages of postnatal ontogeny. This character also shows individual variation, including among adults.

Character 33. Position of aperture of canals transmitting the carotid arteries into the hypophysis: posterolateral portion of hypophysis (0), or anterolateral portion of hypophysis (1). This character is from Macrini et al. (2007b; Character 19). There is no variation in how this character is scored for the sample of *Monodelphis domestica* we examined; all specimens exhibit state (0).

Character 34. Cavum epiptericum: confluent with cavum supracochleare (0); or Cavum epiptericum and cavum supracochleare separated by at least a partial bony wall (1). This character is from Wible (1990). The specimen of *Didelphis virginiana* and all of the *Monodelphis domestica* examined here exhibit character state (1).

Character 35. Position of pons relative to root of cranial nerve V: pons lies anterior to root of cranial nerve V (0); or pons lies wholly posterior to the root of cranial nerve V (1). This character is modified from Macrini (2006; Character 28). This character cannot be evaluated on either endocasts of *Monodelphis domestica* or *Didelphis virginiana* because the pons is not visible on any of these. However, dissections reveal that the pons lies anterior to the root of cranial nerve V on the hindbrain for all *M. domestica* examined.

Summary of Variation Among Endocranial Characters and Implications for this Study

Character 13 was not applicable for endocasts of *Monodelphis domestica*. Of the remaining 34 characters, 13 (~38%) showed some sort of intraspecific variation (ontogenetic, individual, or both) and 21 (~62%) were not variable. Two of 34 characters (~6%) showed only individual variation, four (~12%) showed only ontogenetic variation, and seven (~21%) showed both types of variation.

Examined in a different way, nine of the 35 characters are quantitative and the remaining 26 are qualitative. Of the nine quantitative characters, one only shows variation between individuals of comparable age, seven show both ontogenetic and individual variation, and one shows no variation. Unsurprisingly, ~89% of the quantitative endocranial characters show some sort of variation. In contrast, only ~21% of the qualitative characters show some sort of variation. Of the 26 qualitative characters, one only shows individual variation, four only show ontogenetic variation, 21 show no variation at all, and one character is not applicable to the endocranial cavity of *Monodelphis domestica*.

These results indicate that both ontogenetic and individual variation affect how endocranial characters are scored for phylogenetic analysis, at least for the taxon *Monodelphis domestica*. However, the taxonomic extent to which these results are applicable is unclear at this point (e.g., Are these characters variable for all marsupials, all therians, or all mammals?). Further study is required to address this question.

But assuming that the polymorphism of at least some endocranial characters is more widespread than the species *Monodelphis domestica*, individual variation should be addressed by examination of multiple specimens of each taxon. Ontogenetic variation can be dealt with either by only scoring characters from individuals of comparable age (e.g., only adults) or by examining growth series for each taxon. Either approach requires a careful assessment of the ontogeny of each specimen. It is important to mention that only three characters (3, 31, 32), all of which are quantitative, show variation among our sample of adult individuals. Therefore, if only qualitative characters are examined on adult specimens of *M. domestica*, none of the characters is variable.

Individual and ontogenetic variation of endocranial characters can and should certainly be examined in other extant mammals; in particular, eutherians and monotremes. However, obtaining multiple individuals of fossil taxa is not always feasible. For instance, several key Mesozoic mammals and nonmammalian cynodonts are represented by a sample size of one and therefore variation cannot be evaluated. Even when multiple individuals of a fossil taxon are available, preservation biases further limit sample sizes. Specimens with missing, damaged, or distorted braincases will have at least some missing data for endocranial characters. This is illustrated by the distortion of the hypophyseal fossa in one of the Day 27 individuals of *Monodelphis domestica* (TMM M-7595). This being said, there are opportunities to examine multiple individuals of the same species of fossil mammal. For example, several dozen natural endocasts of the

Eocene oreodont *Bathygenys reevesi* are known from a single locality in West Texas (Wilson, 1971; Macrini, unpublished observation).

CONCLUDING REMARKS

Now that intraspecific variation of endocasts of *Monodelphis domestica* is documented, endocranial characters scored for this taxon should be dealt with accordingly in phylogenetic analyses. Possible treatments of polymorphic characters in phylogenetic analyses include (but are not limited to) ignoring these characters altogether ("fixed-only" method), breaking up terminal taxa into nonvariant subunits, coding only the most common polymorphic state, using a step matrix to order polymorphic states, and incorporating frequency data on polymorphic characters (Campbell and Frost, 1993; Wiens, 2000). These different coding methods are compared in the literature (Campbell and Frost, 1993; Wiens, 1995, 1998, 1999, 2000; Kornet and Turner, 1999; Voss and Jansa, 2003). Although different authors favor different methods, it is clear that the fixed-only method is the least accurate when the true phylogeny is known from simulation studies or congruence studies in which the same clades are recovered by a number of different data sets (Wiens, 1999, 2000).

In summary, we provide answers to the three questions we investigated in this study. First, based on this particular sample of *Monodelphis domestica*, the ontogeny of a specimen affects how phylogenetic characters pertaining to the endocranial cavity are scored. Second, individual variation is noticeable in this sample of endocasts of *M. domestica*; therefore, multiple individuals of this taxon should be examined when conducting phylogenetic analyses of endocranial characters. Third, the brain growth trajectory of *M. domestica* varies significantly from the brain allometry trajectory determined from a sample of adult specimens of several didelphid species. This suggests that juvenile specimens of a particular mammalian taxon might have a significantly different brain size relative to body size than an adult of that same species. Therefore, the ontogeny of an individual should be taken into consideration for EQ studies.

In closing, further studies such as this should be conducted to determine the taxonomic extent of significant ontogenetic and individual variation of these endocranial characters. Multiple individuals of a taxon should be examined, if possible, when scoring endocranial characters for phylogenetic analysis. This article is only a preliminary study of intraspecific variation in mammalian endocasts; subsequent studies are planned to examine variation in extant eutherians and monotremes as well as among taxa of fossil mammals. Other types of intraspecific variation (e.g., sexual dimorphism) should also be examined on endocasts of *Monodelphis domestica* and other mammalian taxa in the future.

ACKNOWLEDGMENTS

Authors thank Cambria Denison, Matt Colbert, and Rich Ketcham of UTCT for scanning all specimens used in this study. Authors thank Darrin Lunde, Teresa Pacheco, and Nancy Simmons for access to specimens of *Monodelphis domestica* in the Department of Mammalogy of the AMNH. Authors also thank Chris J. Bell, Dave Cannatella, Zhe-Xi Luo, Marcelo Sánchez-Villagra, Jim Sprinkle, and an anonymous reviewer for critical comments on earlier versions of this manuscript.

LITERATURE CITED

Aitkin L, Cochran S, Frost S, Martsi-McClintock A, Masterton B. 1997. Features of the auditory development of the short-tailed Brazilian opossum, *Monodelphis domestica*: Evoked responses, neonatal vocalizations and synapses in the inferior colliculus. Hear Res 113:69–75.

Allen H. 1882. On a revision of the ethmoid bone in the Mammalia, with special reference to the description of this bone and of the sense of smelling in the Cheiroptera. Bull Mus Comp Zool 10:135–164.

Bauchot R, Stephan H. 1967. Encéphales et moulages endocraniens de quelques insectivores et primates actuels. In: Problemes actuels de paleontologie (Évolution des Vertébrés): Colloques Internationaux du Centre National de la Recherche Scientifique. Paris, France, 6–11 June 1966. Editions du Centre National de la Recherche Scientifique 163:575–586.

Bell CJ, Gauthier J. 2002. North American Quaternary Squamata: Reevaluation of the stability hypothesis. J Vertebr Paleontol 22(Suppl 3):35A.

Bever GS. 2005. Variation in the ilium of North American *Bufo* (Lissamphibia; Anura) and its implications for species-level identification of fragmentary anuran fossils. J Vertebr Paleontol 25:548–560.

Bever GS, Rowe T, Ekdale EG, Macrini TE, Colbert MW, Balanoff AM. 2005. Comment on "Independent origins of middle ear bones in Monotremes and Therians" (I). Science 309:1492a.

Brochu CA. 2000. A digitally-rendered endocast for *Tyrannosaurus rex*. J Vertebr Paleontol 20:1–6.

Brückner G, Härtig W, Seeger J, Rübsamen R, Reimer K, Brauer K. 1998. Cortical perineuronal nets in the gray short-tailed opossum (*Monodelphis domestica*): A distribution pattern contrasting with that shown in placental mammals. Anat Embryol 197:249–262.

Brunjes PC, Jazaeri A, Sutherland MJ. 1992. Olfactory bulb organization and development in *Monodelphis domestica* (grey short-tailed opossum). J Comp Neurol 320:544–554.

Buchholtz EA, Seyfarth E-A. 1999. The gospel of the fossil brain: Tilly Edinger and the science of paleoneurology. Brain Res Bull 48:351–361.

Butler AB, Hodos W. 1996. Comparative Vertebrate Neuroanatomy: Evolution and Adaptation. New York: Wiley-Liss. 514 pp.

Campbell JA, Frost DR. 1993. Anguid lizards of the genus *Abronia*: Revisionary notes, descriptions of four new species, a phylogenetic analysis, and key. Bull Am Mus Nat Hist 216:1–121.

Carlson WD, Rowe T, Ketcham RA, Colbert MW. 2003. Geological applications of high-resolution X-ray computed tomography in petrology, meteoritics and palaeontology. In: Mees FR, Swennen R, Van Geet M, Jacobs P, editors. Applications of X-ray Computed Tomography in the Geosciences, Vol. 215. London: Geological Society. pp 7–22.

Clark CT, Smith KK. 1993. Cranial osteogenesis in *Monodelphis domestica* (Didelphidae) and *Macropus eugenii* (Macropodidae). J Morphol 215:119–149.

Colbert MW, Racicot R, Rowe T. 2005. Anatomy of the cranial endocast of the bottlenose dolphin *Tursiops truncatus*, based on HRXCT. J Mammal Evol 12:195–207.

Cothran EG, Aivaliotis MJ, VandeBerg JL. 1985. The effects of diet on growth and reproduction in gray short-tailed opossums *Monodelphis domestica*. J Exp Zool 236:103–114.

Denison C, Carlson WD, Ketcham RA. 1997. Three-dimensional quantitative textural analysis of metamorphic rocks using high-resolution computed X-ray tomography, Part 1: Methods and techniques. J Metamorph Geol 15:29–44.

de Queiroz K, Gauthier J. 1990. Phylogeny as a central principle in taxonomy: Phylogenetic definitions of taxon names. Syst Zool 39:307–322.

Dom R, Fisher BL, Martin GF. 1970. The venous system of the head and neck of the opossum (*Didelphis virginiana*). J Morphol 132:487–496.

Dozo MT. 1989. Estudios paleoneurologicos en Didelphidae extinguidos (Mammalia, Marsupialia) de la Formación Chapadmalal (Plioceno tardío), Provincia de Buenos Aires, Argentina. Ameghiniana 26:43–54.

Dozo MT. 1994. Estudios paleoneurologicos en marsupiales "carnivoros" extinguidos de America del Sur: Neuromorfologia y encephalization. Mastozoología Neotropical 1:5–16.

Edinger T. 1942. The pituitary body in giant animals fossil and living: A survey and a suggestion. Q Rev Biol 17:31–45.

Edinger T. 1948. Evolution of the horse brain. Geol Soc Am Memoir 25:1–177.

Edinger T. 1949. Paleoneurology versus comparative brain anatomy. Confin Neurol 9:5–24.

Edinger T. 1955. Hearing and smell in cetacean history. Monatsschr Psychiatr Neurol 129:37–58.

Edinger T. 1964. Midbrain exposure and overlap in mammals. Am Zool 4:5–19.

Edinger T. 1975. Paleoneurology 1804–1966. An annotated bibliography. Ergeb Anat Entwicklungsgesch 49:1–258.

Eisenberg JF, Wilson DE. 1981. Relative brain size and demographic strategies in didelphid marsupials. Am Nat 118:1–15.

Farrand WR. 1961. Frozen mammoths and modern geology. Science 133:729–735.

Felsenstein J. 1985. Phylogenies and the comparative method. Am Nat 125:1–15.

Filan S. 1991. Development of the middle ear region in *Monodelphis domestica* (Marsupialia, Didelphidae): Marsupial solutions to an early birth. J Zool Lond 25:577–588.

Flynn JJ, Wyss AR. 1999. New marsupials from the Eocene-Oligocene transition of the Andean main range, Chile. J Vertebr Paleontol 19:533–549.

Franzosa JW. 2004. Evolution of the brain in Theropoda (Dinosauria), PhD Dissertation. Austin: University of Texas at Austin. 357 pp.

Franzosa JW, Rowe T. 2005. Cranial endocast of the Cretaceous theropod dinosaur *Acrocanthosaurus atokensis*. J Vertebr Paleontol 25:859–864.

Guthrie RD. 1990. Frozen Fauna of the Mammoth Steppe: The Story of Blue Babe. Chicago, Illinois: University of Chicago Press.323 pp.

Haight JR, Murray PF. 1981. The cranial endocast of the early Miocene marsupial, *Wynyardia bassiana*: An assessment of taxonomic relationships based upon comparisons with Recent forms. Brain Behav Evol 19:17–36.

Haight JR, Nelson JE. 1987. A brain that doesn't fit its skull: A comparative study of the brain and endocranium of the koala, *Phascolarctos cinereus* (Marsupialia: Phascolarctidae). In: Archer M, editor. Possums and Opossums: Studies in Evolution, Vol. 1. Chipping Norton, New South Wales, Australia: Surrey Beatty and Sons Pty Limited. pp 331–352.

Harvey PH, Krebs JR. 1990. Comparing brains. Science 249: 140–146.

Hilton EJ, Bemis WE. 1999. Skeletal variation in shortnose sturgeon (*Acipenser brevirostrum*) from the Connecticut River: Implications for comparative osteological studies of fossil and living fishes. In: Arratia G, Schultze H-P, editors. Systematics and Fossil Record. München, Germany: Verlag Dr. Friedrich Pfeil. pp 69–94.

Holloway RL, Broadfield DC, Yuan MS. 2004. The Human Fossil Record, Vol. 3: Brain Endocasts—The Paleoneurological Evidence. New York: Wiley-Liss. 315 pp.

Horovitz I, Sánchez-Villagra MR. 2003. A morphological analysis of marsupial mammal higher-level phylogenetic relationships. Cladistics 19:181–212.

Hurlburt GR. 1996. Relative brain size in Recent and fossil amniotes: Determination and interpretation, PhD Dissertation. Toronto: University of Toronto. 250 pp.

Jansa SA, Voss RS. 2000. Phylogenetic studies on didelphid marsupials. I. Introduction and preliminary results from nuclear IRBP gene sequences. J Mammal Evol 7:43–77.

Jansa SA, Voss RS. 2005. Phylogenetic relationships of the marsupial genus *Hyladelphys* based on nuclear gene sequences and morphology. J Mammal 86:853–865.

Jansa SA, Forsman JF, Voss RS. 2006. Different patterns of selection on the nuclear genes IRBP and DMP-1 affect the efficiency but not the outcome of phylogeny estimation for didelphid marsupials. Mol Phylogenet Evol 38:363–380.

Jerison HJ. 1973. Evolution of the Brain and Intelligence. New York: Academic Press. 482 pp.

Jerison HJ. 1979. The evolution of diversity in brain size. In: Hahn ME, Jensen C, Dudek BC, editors. Development and Evolution of Brain Size: Behavioral Implications. New York: Academic Press. pp 29–57.

Jerison HJ. 1991. Fossil brains and the evolution of the neocortex. In: Finlay BL, Innocenti G, Scheich H, editors. The Neocortex: Ontogeny and Phylogeny (NATO Advanced Science Institutes Series A: Life Sciences, Vol. 200). New York: Plenum. pp 5–19.

Johnson JI. 1977. Central nervous system of marsupials. In: Hunsaker D, editor. The Biology of Marsupials. New York: Academic Press. pp 157–278.

Johnson JI, Switzer RC, Kirsch JAW. 1982a. Phylogeny through brain traits: Fifteen characters which adumbrate mammalian genealogy. Brain Behav Evol 20:72–83.

Johnson JI, Switzer RC, Kirsch JAW. 1982b. Phylogeny through brain traits: The distribution of categorizing characters in contemporary mammals. Brain Behav Evol 20:97–117.

Johnson JI, Kirsch JAW, Reep RL, Switzer RC. 1994. Phylogeny through brain traits: More characters for the analysis of mammalian evolution. Brain Behav Evol 43:319–347.

Kielan-Jaworowska Z. 1983. Multituberculate endocranial casts. Palaeovertebrata 13:1–12.

Kielan-Jaworowska Z. 1984. Evolution of the therian mammals in the late Cretaceous of Asia. VI. Endocranial casts of eutherian mammals. Palaeontol Pol 46:157–171.

Kielan-Jaworowska Z. 1986. Brain evolution in Mesozoic mammals. In: Flanagan KM, Lillegraven JA, editors. Vertebrates, Phylogeny, and Philosophy. Contributions to Geology, Special Paper 3. Laramie: University of Wyoming. pp 21–34.

Kielan-Jaworowska Z, Lancaster TE. 2004. A new reconstruction of multituberculate endocranial casts and encephalization quotient of *Kryptobaatar*. Acta Palaeontol Pol 49:177–188.

Kielan-Jaworowska Z, Cifelli RL, Luo Z-X. 2004. Mammals from the Age of Dinosaurs: Origin, Evolution, and Structure. New York: Columbia University Press. 630 pp.

Kirsch JAW. 1983. Phylogeny through brain traits: Objectives and method. Brain Behav Evol 22:53–59.

Kirsch JAW, Johnson JI. 1983. Phylogeny through brain traits: Trees generated by neural characters. Brain Behav Evol 22: 60–69.

Kirsch JAW, Johnson JI, Switzer RC. 1983. Phylogeny through brain traits: The mammalian family tree. Brain Behav Evol 22:70–74.

Kornet DJ, Turner H. 1999. Coding polymorphism for phylogenetic reconstruction. Syst Biol 48:365–379.

Krabbe KH. 1942. Studies on the Morphogenesis of the Brain in Lower Mammals. Morphogenesis of the Vertebrate Brain II. Copenhagen: Einar Munksgaard. 124 pp.
Kraus DH, Fadem BH. 1987. Reproduction, development, and physiology of the gray short-tailed opossum (*Monodelphis domestica*). Lab Anim Sci 37:478–482.
Kühn HJ, Zeller U. 1987. The cavum epiptericum in monotremes and therian mammals. In: Kühn HJ, Zeller U, editors. Mammalia Depicta, Morphogenesis of the Mammalian Skull. Hamburg: Paul Parey Verlag. pp 51–70.
Larsell O. 1936. The development and morphology of the cerebellum in the opossum. J Comp Neurol 63:251–291.
Larsson HCE, Sereno PC, Wilson JA. 2000. Forebrain enlargement among nonavian dinosaurs. J Vertebr Paleontol 20:615–618.
Loo YT. 1930. The forebrain of the opossum, *Didelphis virginiana*. J Comp Neurol 51:13–64.
Luo Z-X, Wible JR. 2005. A late Jurassic digging mammal and early mammalian diversity. Science 308:103–107.
Luo Z-X, Cifelli RL, Kielan-Jaworowska Z. 2001a. Dual origin of tribosphenic mammals. Nature 409:53–57.
Luo Z-X, Crompton AW, Sun A-L. 2001b. A new mammaliaform from the early Jurassic and evolution of mammalian characteristics. Science 292:1535–1540.
Luo Z-X, Kielan-Jaworowska Z, Cifelli RL. 2002. In quest for a phylogeny of Mesozoic mammals. Acta Palaeontol Pol 47:1–78.
Luo Z-X, Ji Q, Wible JR, Yuan C-X. 2003. An early Cretaceous tribosphenic mammal and metatherian evolution. Science 302:1934–1940.
Lyras GA, van der Geer AAE. 2003. External brain anatomy in relation to the phylogeny of Caninae (Carnivora: Canidae). Zool J Linn Soc 138:505–522.
MacLeod N, Forey PL, editors. 2002. Morphology, Shape and Phylogeny. New York: Taylor and Francis. 308 pp.
Macrini TE. 2000. High resolution X-ray computed tomography (CT) of the skull of an extant opossum (*Monodelphis domestica*) and a comparison of its ontogeny to synapsid phylogeny, MS Thesis. Austin: University of Texas at Austin. 158 pp.
Macrini TE. 2002. Quantitative comparison of ontogenetic and phylogenetic character changes in the synapsid mandible and auditory region. J Mammal Evol 9:185–207.
Macrini TE. 2004. *Monodelphis domestica*. Mammalian Species 760:1–8.
Macrini TE. 2006. The evolution of endocranial space in mammals and non-mammalian cynodonts, PhD Dissertation. Austin: University of Texas at Austin. 278 pp.
Macrini TE, Rowe T, Archer M. 2006. Description of a cranial endocast from a fossil platypus, *Obdurodon dicksoni* (Monotremata, Ornithorhynchidae), and the relevance of endocranial characters to monotreme monophyly. J Morphol 267: 1000–1015.
Macrini TE, Muizon C, Cifelli RL, Rowe T. 2007a. Digital cranial endocast of *Pucadelphys andinus*, a Paleocene metatherian. J Vertebr Paleontol 27:99–107.
Macrini TE, Rougier GW, Rowe T. 2007b. Description of a cranial endocast from the fossil mammal *Vincelestes neuquenianus* (Theriiformes) and its relevance to the evolution of endocranial characters in therians. Anat Rec 290:875–892.
Maier W. 1987a. The ontogenetic development of the orbitotemporal region of the skull of *Monodelphis domestica* (Didelphidae, Marsupialia), and the problem of the mammalian alisphenoid. In: Kühn HJ, Zeller U, editors. Mammalia Depicta, Morphogenesis of the Mammalian Skull. Hamburg: Paul Parey Verlag. pp 71–90.
Maier W. 1987b. Der Processus angularis bei *Monodelphis domestica* (Didelphidae: Marsupialia) und seine Beziehungen zum Mittelohr: eine ontogenetische und evolutionmorphologische Untersuchung. Gegen Morphol Jb 133:123–161.
Maier W. 1990. Phylogeny and ontogeny of mammalian middle ear structures. Neth J Zool 40:55–74.
Marsh OC. 1884. Dinocerata. A monograph of an extinct order of gigantic mammals. US Geol Surv 10:1–237.
Maunz M, German RZ. 1996. Craniofacial heterochrony and sexual dimorphism in the short-tailed opossum (*Monodelphis domestica*). J Mammal 77:992–1005.
Maunz M, German RZ. 1997. Ontogeny and limb bone scaling in two New World marsupials, *Monodelphis domestica* and *Didelphis virginiana*. J Morphol 231:117–130.
Miguel C de, Henneberg M. 1998. Encephalization of the koala, *Phascolarctos cinereus*. Aust Mammal 20:315–320.
Nesterova TB, Isaenko AA, Matveeva NM, Shilov AG, Rubtsova NB, Vorobieva NV, Rubtsova NV, VandeBerg JL, Zakian SM. 1997. Novel strategies for eutherian-marsupial somatic cell hybrids: Mapping the genome of *Monodelphis domestica*. Cytogenet Cell Genet 76:115–122.
Nieuwenhuys R, Ten Donkelaar HJ, Nicholson C. 1998. The Central Nervous System of Vertebrates (3 vols). Berlin: Springer Verlag. 2219 pp.
Northcutt RG. 1984. Evolution of the vertebrate central nervous system: Patterns and processes. Am Zool 24:701–716.
Northcutt RG. 1985. The brain and sense organs of the earliest vertebrates: Reconstruction of a morphotype. In: Foreman RE,Gorbman A, Dodd JM, Olsson R, editors. Evolutionary Biology of Primitive Fishes. New York: Plenum. pp 81–112.
Novacek MJ. 1982. The brain of *Leptictis dakotensis*, an Oligocene leptictid (Eutheria: Mammalia) from North America. J Paleontol 56:1177–1186.
Novacek MJ. 1986. The skull of leptictid insectivorans and the higher-level classification of eutherian mammals. Bull Am Mus Nat Hist 183:1–112.
Novacek MJ. 1993. Patterns of diversity in the mammalian skull. In: Hanken J, Hull BK, editors. The Skull, Vol. 2: Patterns of Structural and Systematic Diversity. Chicago: University of Chicago Press. pp 438–545.
Nowak RM. 1999. Walker's Mammals of the World, Vol. 1. Baltimore, MD: Johns Hopkins University Press. 6th ed., 836 pp.
Owen R. 1837. On the structure of the brain in marsupial animals. Phil Trans R Soc Lond 127:87–96.
Owen R. 1868. On the Anatomy of Vertebrates, Vol. III: Mammals. London: Longmans/Green and Co. 915 pp.
Pagel MD, Harvey PH. 1988. The taxon-level problem in the evolution of mammalian brain size: Facts and artifacts. Am Nat 132:344–359.
Quiroga JC. 1978. El encefalo de *Borhyaena fera* (Mammalia-Marsupialia). Estudio preliminar sobre las areas corticales en dos marsupiales extinguidos. Publicaciones del Museo Municipal de Ciencias Naturales de Mar del Plata "Lorenzo Scaglia" 2:191–197.
Quiroga JC, Dozo JC. 1988. The brain of *Thylacosmilus atrox*. Extinct South American saber-tooth carnivore marsupial. J Hirnforsch 29:573–586.
Radinsky L. 1968a. A new approach to mammalian cranial analysis, illustrated by examples of prosimian primates. J Morphol 124:167–180.
Radinsky L. 1968b. Evolution of somatic sensory specialization in otter brains. J Comp Neurol 134:495–505.
Radinsky L. 1973a. Are stink badgers skunks? Implications of neuroanatomy for mustelid phylogeny. J Mammal 54:585–593.
Radinsky L. 1973b. Evolution of the canid brain. Brain Behav Evol 7:169–202.
Radinsky L. 1976. The brain of *Mesonyx*, a middle Eocene mesonychid condylarth. Fieldiana Geol 33:323–337.
Radinsky L. 1977. Brains of early carnivores. Paleobiology 3:333–349.
Reimer K. 1996. Ontogeny of hearing in the marsupial *Monodelphis domestica*, as revealed by brainstem auditory evoked potentials. Hear Res 92:143–150.
Robinson ES, VandeBerg JL, Hubbard GB, Dooley TP. 1994. Malignant melanoma in UV-irradiated laboratory opossums: Initiation in suckling young, metastasis in adults, and xenograft behavior in nude mice. Cancer Res 54:5986–5991.
Roth G, Wullimann MF, editors. 2001. Brain Evolution and Cognition. New York: Wiley. 597 pp.

Rougier GW, Wible JR, Novacek MJ. 1998. Implications of *Deltatheridium* specimens for early marsupial history. Nature 396:459–463.

Rowe T. 1988. Definition, diagnosis, and origin of Mammalia. J Vertebr Paleontol 8:241–264.

Rowe T. 1996a. Brain heterochrony and the evolution of the mammalian middle ear. In: Ghiselin M, Pinna G, editors. New Perspectives on the History of Life. Memoir 20. San Francisco: California Academy of Sciences. pp 71–95.

Rowe T. 1996b. Coevolution of the mammalian middle ear and neocortex. Science 273:651–654.

Rowe T, Carlson W, Bottorff W. 1995. Thrinaxodon: Digital Atlas of the Skull (CD-ROM), 2nd ed. Austin: University of Texas Press.

Rowe TB, Eiting TP, Macrini TE, Ketcham RA. 2005. Organization of the olfactory and respiratory skeleton in the nose of the gray short-tailed opossum *Monodelphis domestica*. J Mammal Evol 12:303–336.

Sánchez-Villagra MR. 2001. Ontogenetic and phylogenetic transformations of the vomeronasal complex and nasal floor elements in marsupial mammals. Zool J Linn Soc 131:459–479.

Sánchez-Villagra MR. 2002. The cerebellar paraflocculus and the subarcuate fossa in *Monodelphis domestica* and other marsupial mammals: Ontogeny and phylogeny of a brain-skull interaction. Acta Theriol 47:1–14.

Sánchez-Villagra MR, Sultan F. 2002. The cerebellum at birth in therian mammals, with special reference to rodents. Brain Behav Evol 59:101–113.

Sánchez-Villagra MR, Wible JR. 2002. Patterns of evolutionary transformation in the petrosal bone and some basicranial features in marsupial mammals, with special reference to didelphids. J Zool Syst Evol Res 40:26–45.

Sánchez-Villagra MR, Gemballa S, Nummela S, Smith KK, Maier W. 2002. Ontogenetic and phylogenetic transformations of the ear ossicles in marsupial mammals. J Morphol 251: 219–238.

Saunders NR, Adam E, Reader M, Møllgård K. 1989. *Monodelphis domestica* (grey short-tailed opossums): An accessible model for studies of early neocortical development. Anat Embryol 180:227–236.

Shoshani J, Kupsky WJ, Marchant GH. 2006. Elephant brain part I: Gross morphology, functions, comparative anatomy, and evolution. Brain Res Bull 70:124–157.

Simpson GG. 1927. Mesozoic Mammalia. IX. The brain of Jurassic mammals. Am J Sci 214:259–268.

Simpson GG. 1937. Skull structure of the Multituberculata. Bull Am Mus Nat Hist 73:727–763.

Sokal RR, Rohlf FJ. 1998. Biometry: The Principles and Practice of Statistics in Biological Research. New York: WH Freeman. 887 pp.

Striedter GF. 2005. Principles of Brain Evolution. Sunderland, Massachusetts: Sinauer Associates. 436 pp.

Taylor J, Rühli FJ, Brown G, Miguel C de, Henneberg M. 2006. MR imaging of brain morphology, vascularisation and encephalization in the koala. Aust Mammal 28:243–247.

Thiele K. 1993. The holy grail of the perfect character: The cladistic treatment of morphometric data. Cladistics 9:275–304.

VandeBerg JL. 1990. The gray short-tailed opossum (*Monodelphis domestica*) as a model didelphid species for genetic research. Aust J Zool 37:235–247.

VandeBerg JL. 1999. The laboratory opossum (*Monodelphis domestica*). In: Poole T, English P, editors. UFAW Handbook on the Care and Management of Laboratory Animals. Oxford, UK: Blackwell Science. pp 193–209.

VandeBerg JL, Robinson ES. 1997. The laboratory opossum (*Monodelphis domestica*) in biomedical research. In: Saunders N, Hinds L, editors. Marsupial Biology. Recent Research, New Perspectives. Sydney: University of New South Wales Press. pp 238–253.

VandeBerg JL, Williams-Blangero S, Hubbard GB, Ley RD, Robinson ES. 1994. Genetic analysis of ultraviolet radiation-induced skin hyperplasia and neoplasia in a laboratory marsupial model (*Monodelphis domestica*). Arch Dermatol Res 268:12–17.

van Nievelt AFH, Smith KK. 2005. Tooth eruption in *Monodelphis domestica* and its significance for phylogeny and natural history. J Mammal 86:333–341.

Voris HC. 1928. The arterial supply of the brain and spinal cord of the Virginian opossum (*Didelphis virginiana*). J Comp Neurol 44:403–423.

Voris HC, Hoerr NL. 1932. The hindbrain of the opossum, *Didelphis virginiana*. J Comp Neurol 54:277–355.

Voss RS, Jansa SA. 2003. Phylogenetic studies on didelphid marsupials II. Nonmolecular data and new IRBP sequences: Separate and combined analyses of didelphine relationships with denser taxon sampling. Bull Am Mus Nat Hist 276:1–82.

Wible JR. 1990. Petrosals of late Cretaceous marsupials from North America, and a cladistic analysis of the petrosal in therian mammals. J Vertebr Paleontol 10:183–205.

Wible JR. 2003. On the cranial osteology of the short-tailed opossum *Monodelphis brevicaudata* (Didelphidae, Marsupialia). Ann Carneg Mus 72:137–202.

Wiens J. 1995. Polymorphic characters in phylogenetic systematics. Syst Biol 44:482–500.

Wiens J. 1998. Testing phylogenetic methods with tree congruence: Phylogenetic analysis of polymorphic morphological characters in phrynosomatid lizards. Syst Biol 47:427–444.

Wiens J. 1999. Polymorphism in systematics and comparative biology. Ann Rev Ecol Syst 30:327–362.

Wiens J. 2000. Coding morphological variation within species and higher taxa for phylogenetic analysis. In: Wiens J, editor. Phylogenetic Analysis of Morphological Data. Washington, DC: Smithsonian Institution. pp 115–145.

Williams SL, Laubach R, Genoways HH. 1977. Guide to the management of Recent mammal collections. Carneg Mus Nat Hist Spec Publ 4:1–105.

Wilson JA. 1971. Early Tertiary vertebrate faunas, Vieja Group, Trans-Pecos, Texas: Agriochoeridae and Merycoidodontidae. Bull Tex Mem Mus 18:1–83.

Witmer LM, Chatterjee S, Franzosa J, Rowe T. 2003. Neuroanatomy of flying reptiles and implications for flight, posture and behaviour. Nature 425:950–953.